Insights into earthquake source physics from high-frequency seismology

Yehuda Ben-Zion
University of Southern California

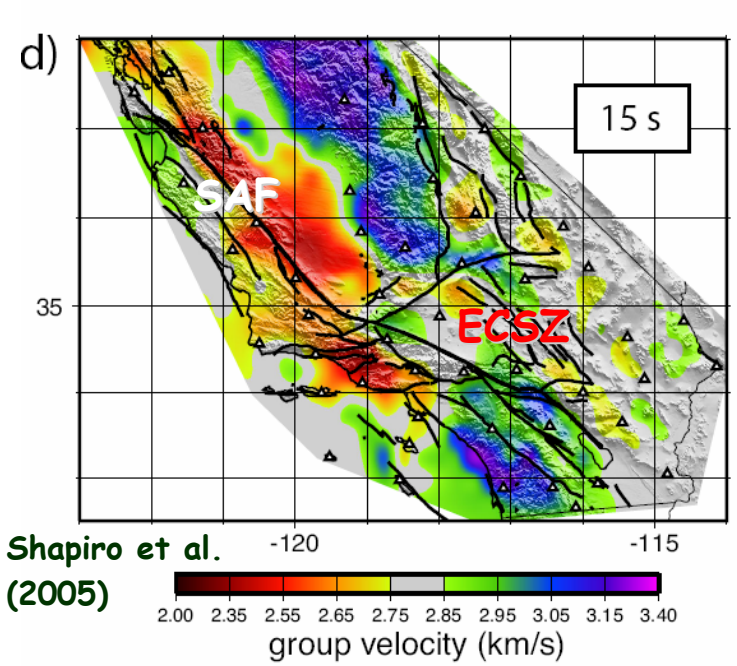

Shapiro et al. (2005)

1957 rupture, Gobi-Altai fault, Mongolia

Immature fault: irregular geometry, distributed dissipative deformation.

Mature fault: approx. planar bimaterial interface, mechanically more efficient.

Theoretical results on small-scale signals with fundamental possible implications to physics of earthquakes and faults in:

1. **Seismic radiation from regions sustaining material damage**
2. **Dynamic rupture on a bimaterial interface**

In-situ tests of the predicted signals requires (very) high-frequency seismology

Seismic radiation from regions sustaining material damage

Yehuda Ben-Zion and Jean-Paul Ampuero
(GJI, 2009)

Seismic Moment:

$$M_{ij} = \int_{V'} c_{ijkl}\varepsilon^{P}_{kl} dV' = \int_{V'} m_{ij} dV'$$

Traditional seismic representation:

$$u_i(\boldsymbol{x},t) = \int_{-\infty}^{t} dt' \int_{V} \frac{\partial G_{ij}(\boldsymbol{x},t;\boldsymbol{x}',t')}{\partial x'_k} \left[m_{jk}(\boldsymbol{x}',t') \right] dV'$$

The co-seismic changes of C_{ijkl} in V', ignored above, can also produce radiation !!!

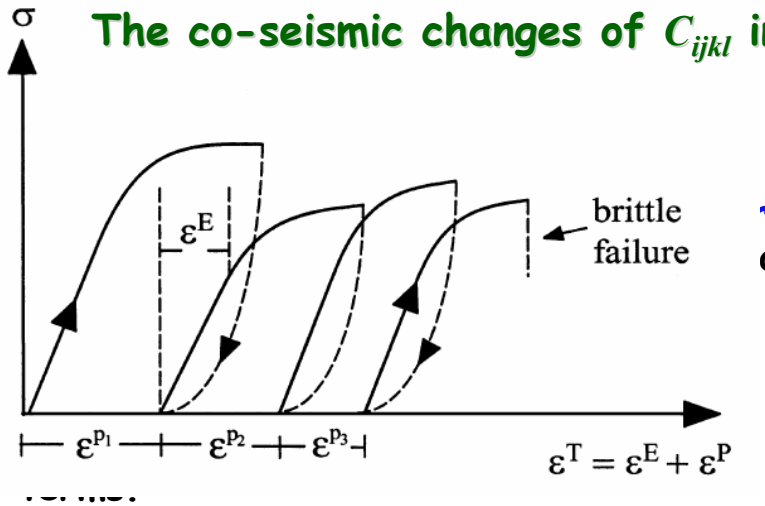

radiation?
orporates
different

Strain energy consideration:

$$\Delta E = \int_{0}^{\varepsilon} \varepsilon_{ij} (c^{f}_{ijkl} - c^{i}_{ijkl}) d\varepsilon_{kl}$$

Basic relations

Total strain has elastic and plastic components: $\varepsilon_{ij}^{t} = \varepsilon_{ij} + p_{ij} = \varepsilon_{ij} + \varepsilon_{ij}^{T}$

Elastic stress-strain in the initial state: $\sigma_{ij} = c_{ijkl}^{i}\varepsilon_{kl}$

and in the final state:

$$\sigma_{ij} = (c_{ijkl}^{i} + \Delta c_{ijkl})(\varepsilon_{kl}^{t} - \varepsilon_{kl}^{T})$$
$$= c_{ijkl}^{i}\varepsilon_{kl}^{t} - c_{ijkl}^{i}\varepsilon_{kl}^{T} + \Delta c_{ijkl}\varepsilon_{kl}$$

The Cauchy equation of motion: $\sigma_{ij,j} + f_i = \rho\ddot{u}_i$

Eq. of M. for final-initial states: $\dfrac{\partial}{\partial x_j}[c_{ijkl}^{i}(\varepsilon_{kl}^{t} - \varepsilon_{kl}^{i})] - \dfrac{\partial}{\partial x_j}(c_{ijkl}^{i}\varepsilon_{kl}^{T}) + \dfrac{\partial}{\partial x_j}(\Delta c_{ijkl}\varepsilon_{kl}) = \rho\ddot{u}_i$

or $\dfrac{\partial}{\partial x_j}(c_{ijkl}^{i}\Delta\varepsilon_{kl}) + f_i^{eff} = \rho\ddot{u}_i$

with incremental strain $\Delta\varepsilon_{kl} = \varepsilon_{kl}^{t} - \varepsilon_{kl}^{i}$

produced by effective body forces with moment and damage source terms

$$f_i^{eff} = -m_{ij,j} + d_{ij,j}$$

$$m_{ij} = c_{ijkl}^{i}\varepsilon_{kl}^{T} \qquad d_{ij} = \Delta c_{ijkl}\varepsilon_{kl}$$

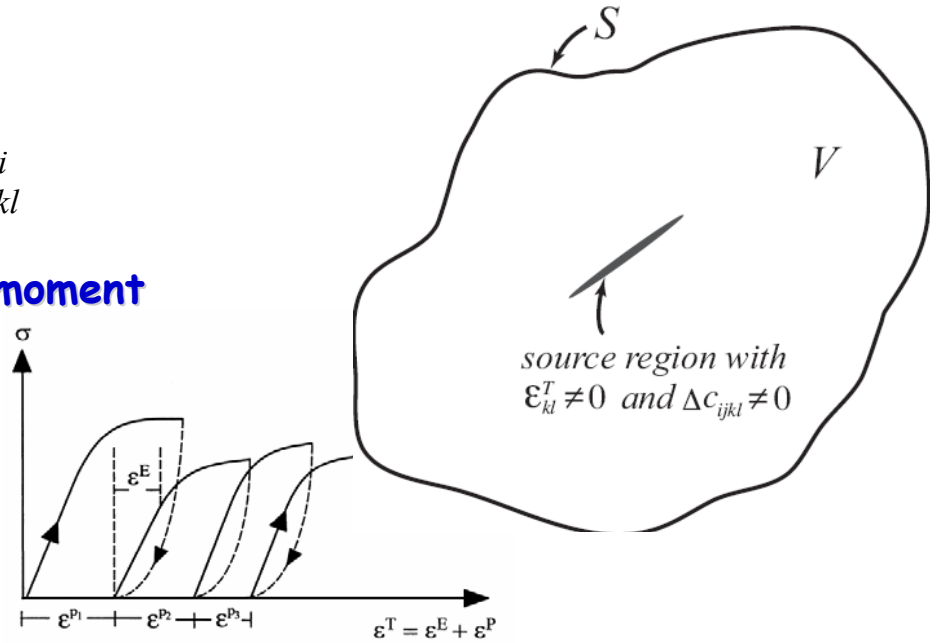

Basic solution

$$u_i(\boldsymbol{x},t) = \int_{-\infty}^{t} dt' \int_V \frac{\partial G_{ij}(\boldsymbol{x},t;\boldsymbol{x}',t')}{\partial x_k'} \left[m_{jk}(\boldsymbol{x}',t') - d_{jk}(\boldsymbol{x}',t') \right] dV'$$

or

$$u_i(\boldsymbol{x},t) = \int_{-\infty}^{t} dt' \int_V \frac{\partial G_{ij}}{\partial x_k'} \left[c^i_{jklm} \varepsilon^T_{lm} \right] dV' - \int_{-\infty}^{\infty} dt' \int_V \frac{\partial G_{ij}}{\partial x_k'} \left[\Delta c_{jklm} \varepsilon_{lm} \right] dV'$$

or $$u_i(\boldsymbol{x},t) = u_i(\boldsymbol{x},t)^{trad} - u_i(\boldsymbol{x},t)^{damage}$$

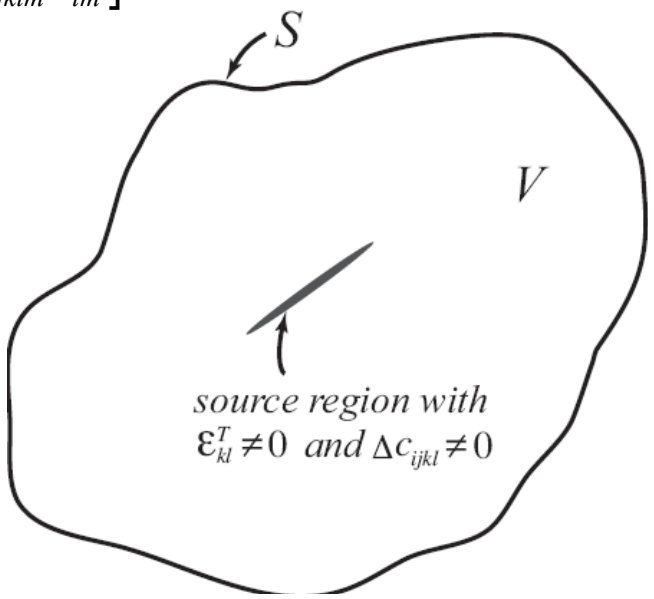

In brittle failure of low porosity rocks and explosions $\Delta C_{ijkl} < 0$ and the damage-related radiation is positive.

In failure of high porosity rocks with compaction bands $\Delta C_{ijkl} > 0$ and the damage-related radiation is negative.

Note that ε in d_{ij} can be order of magnitude larger than ε^T in m_{ij}, so u^{damage} may be larger than u^{trad} !

$$m_{ij} = c^i_{ijkl} \varepsilon^T_{kl}$$

$$d_{ij} = \Delta c_{ijkl} \varepsilon_{kl}$$

Order of magnitude estimates of contributions

$$m \approx \left| c\varepsilon^T \right| \cdot V_1 \approx \Delta\tau \cdot V_1$$

$$d \approx \left| \Delta c\varepsilon \right| \cdot V_2 \approx \left| \Delta c / c \right| \cdot \tau \cdot V_2$$

$$m / d \approx \frac{c}{|\Delta c|} \frac{\Delta\tau}{\tau} V_1 / V_2$$

$$m_{ij} = c^i_{ijkl} \varepsilon^T_{kl}$$

$$d_{ij} = \Delta c_{ijkl} \varepsilon$$

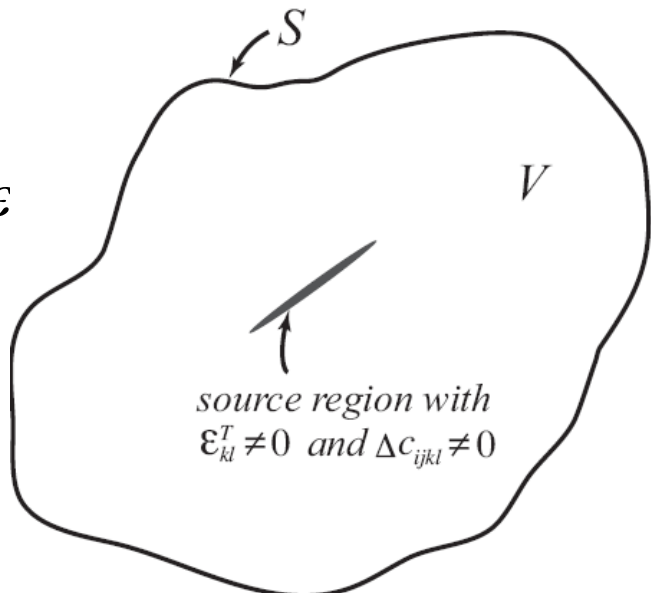

Lab and seismic data suggests that $C/\Delta C$ during brittle failure may be ~0.5 or more (can be ~1 in explosions).

Seismic data suggest that $\Delta\tau/\tau$ during earthquakes is ~0.1-0.2.

Unless $V_1 >> V_2$, $u^{damage} > u^{trad}$!!!

The DC component of u^{damage} can be zero, so much of the radiation is expected to be in high frequency waves!

Order of magnitude estimates with volumes

For crack like ruptures, the moment scales with rupture size *R* as $m \approx \left| c\varepsilon^T \right| \cdot V_1 \approx \Delta\tau \cdot R^3$

The volume associated with the damage process can be written as $V_2 = R^2W$ with *W* = width of yielding zone

From fracture mechanics, $W \approx K^2/(\tau_y - \tau_0)^2$

with stress intensity factor $K \approx \Delta\tau\sqrt{R}$

Thus $W \approx \Delta\tau^2 R/(\tau_y - \tau_0)^2 = R/S^2$

and $m/d \approx \dfrac{c}{|\Delta c|}\dfrac{\Delta\tau}{\tau_0}S^2$

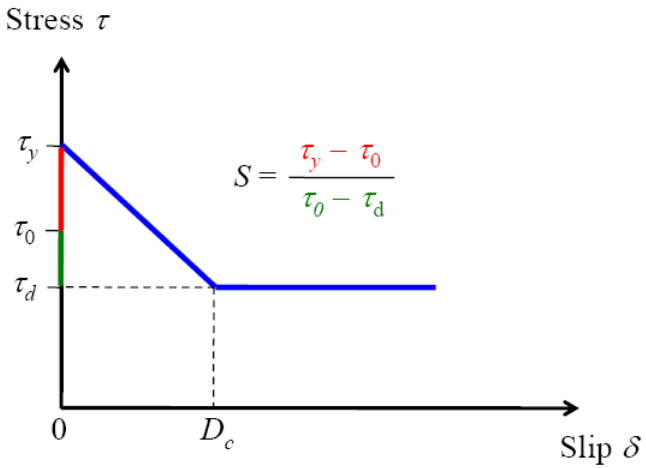

$S < 0.5 \rightarrow$ supershear rupture
$S > 1.5 \rightarrow$ subshear rupture

If $\Delta\tau/\tau_0 \approx 0.1$, $|\Delta c/c| \approx 0.5$, and S = 0.5 (marginal supershear), ***m/d* ≈ 0.3 !!!**

If S = 1.5, 3 and 5 (subshear ruptures), ***m/d* ≈ 2.8, 11, and 31 !!**

If the modulus reduction is 25%, ***m/d* ≈ 5.6, 22, and 62 (still significant) !**

Decomposition analysis: isotropic radiation from $d_{ij} = \Delta c_{ijkl}\varepsilon_{kl}$ **can be > DC component**

Conclusions I

- The ratio of radiation from the moment and damage-related processes scales as $m/d \approx (c/|\Delta c|)(\Delta\tau/\tau)(V_1/V_2)$

- Unless V_1 >> V_2, u^{damage} can be a significant component of the total radiation.

- In fracturing of low porosity rocks and explosions, the radiation from the source to the bulk is larger than traditional estimates based only on the moment contribution. In fracturing of high porosity rocks involving compaction bands, the opposite is true.

- Decomposition analysis suggests that the damage-related radiation can have a significant isotropic component. Much of the radiation of u^{damage} is expected to be in high frequency waves.

- Standard derivations of source parameters map erroneously the damage-related radiation onto moment terms (slip and CLVD)

- Reliable measurements of high frequency waves are needed to test the predictions associated with the damage-related radiation.

Dynamic rupture on a bimaterial interface
(important structural element of large fault zones)

Collaborators:
Theory: Z. Shi, J.P. Ampuero, S. Xu (also earlier Andrews, Huang, Brietzke)
Observations: O. Dor, T. Rockwell, N. Wechsler , I. Zaliapin

SAF, Mojave

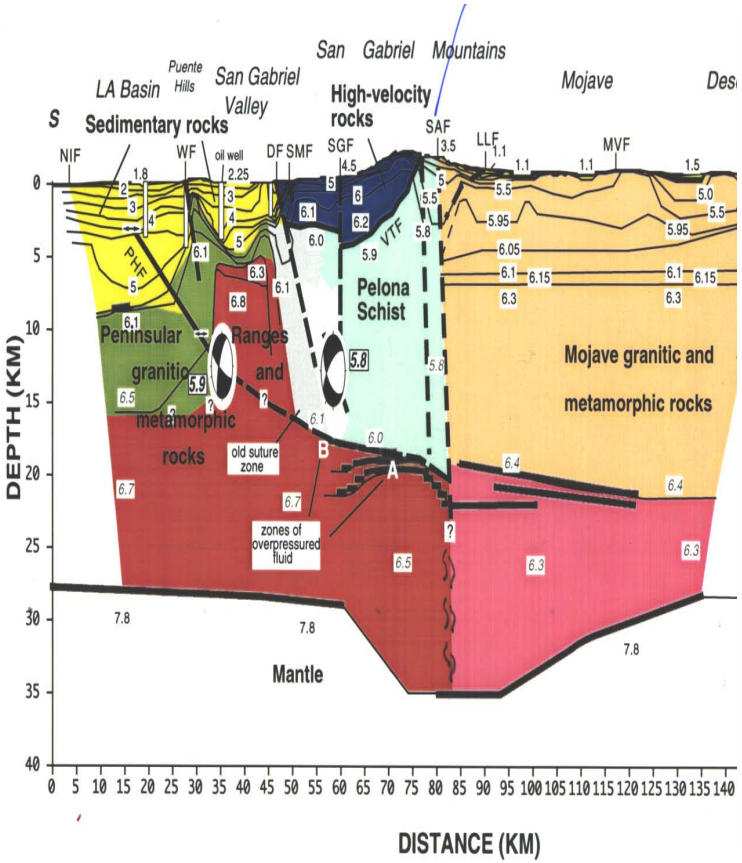

Fuis et al. (2003)

SAF, Parkfield

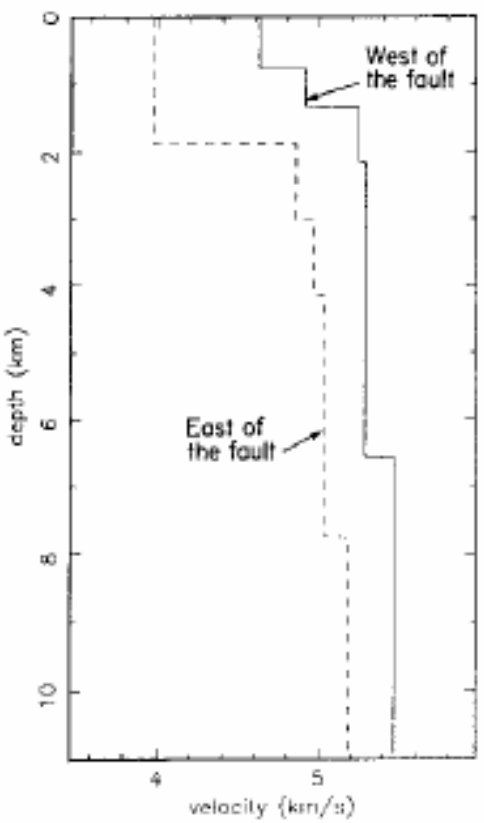

Ben-Zion et al. (1992)

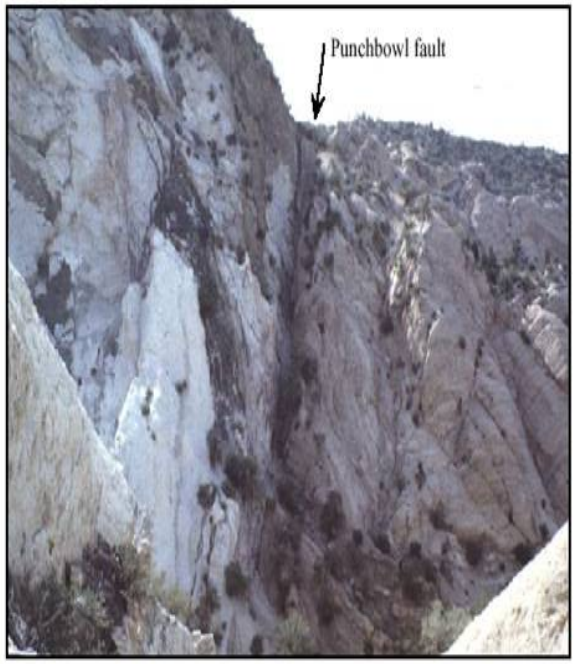

Chester et al. (1993)

Can be relevant to numerous important issues

- Low frictional heat and lack of pervasive melting along large faults
- Short rise-time and high slip velocity in earthquake slip histories
- Suppression of branching and evolution of fault structures
- Expected seismic radiation (and hazard) from large faults
- Earthquake triggering
- Effective constitutive laws of large faults
- …….
- Ruptures along bimaterial interfaces in mines, bottom of glaciers, man-made composite materials, etc.

- Reliable measurements of high frequency waves are needed to test the predictions associated with ruptures on bimaterial interfaces.

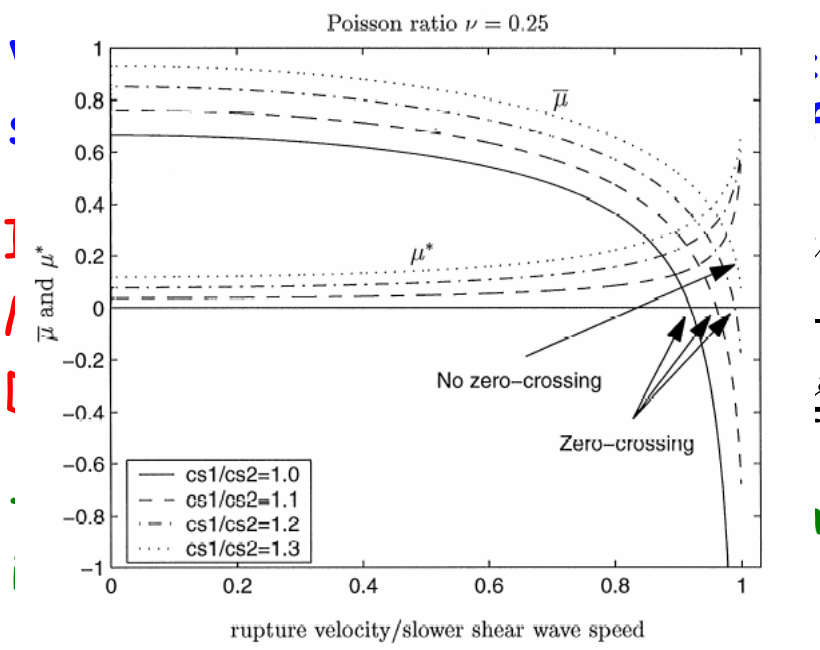

al solution for steady state mode II
face governed by Coulomb friction.

$u(x, y=0^-, t)$

$- ct$

ξ

ie

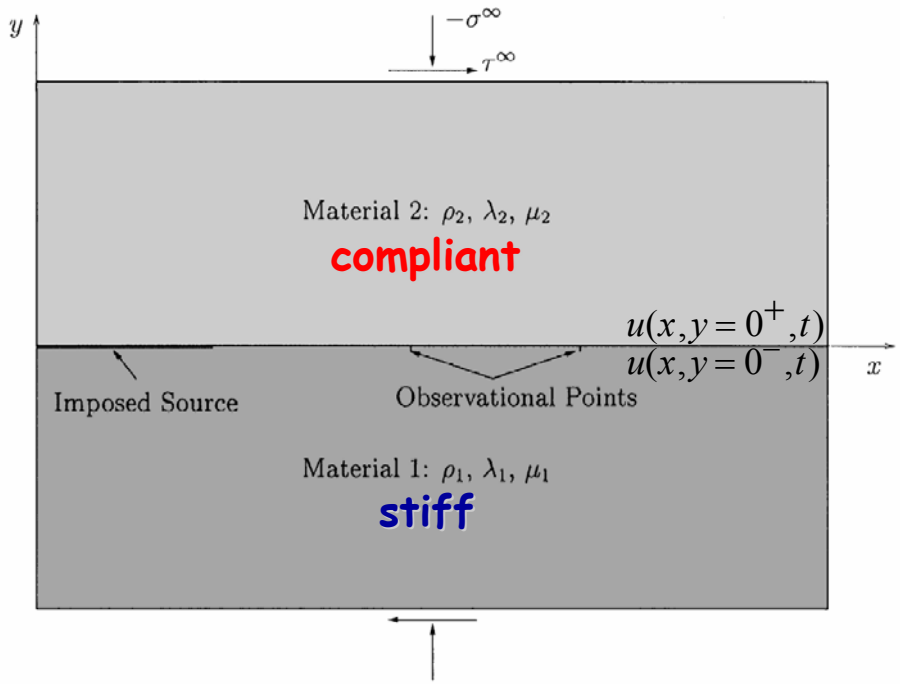

$$\tau(\xi) = \tau^\infty + \frac{\overline{\mu}(c, \Delta\beta)}{\pi} \int_{-\infty}^{\infty} \frac{B(\xi')}{\xi - \xi'} d\xi'$$

$$\sigma(\xi) = \sigma^\infty - \mu^*(c, \Delta\beta) B(\xi)$$

- In a homogeneous solid $\mu^* = 0$; there is no coupling between slip and σ.
- For subsonic rupture on a bimaterial interface in the direction of motion of the compliant solid, $\mu^* > 0$ and σ drops dynamically (producing local dilation).
- In the opposite direction, $\mu^* < 0$ and σ increases dynamically (local compression).
- Adams (1995): The bimaterial effects increase with propagation distance!

Wrinkle-like rupture pulse

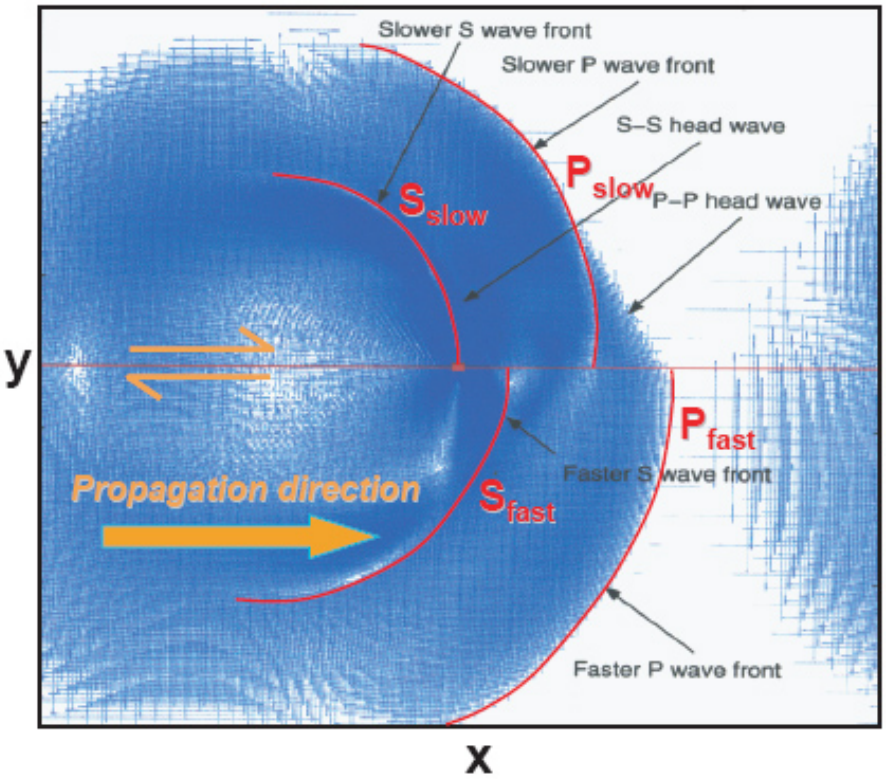

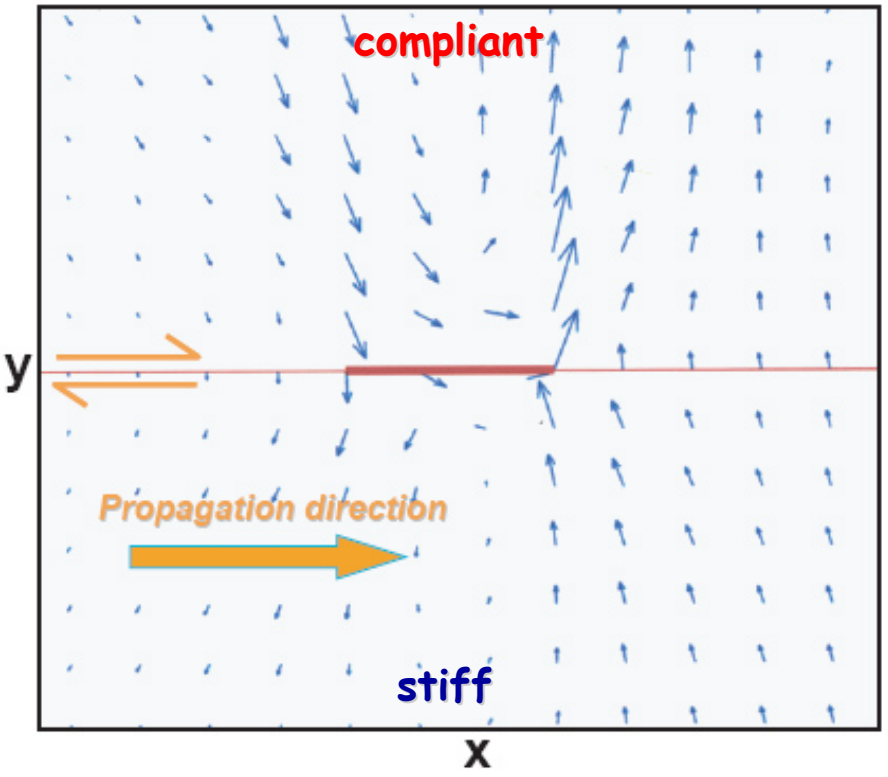

Andrews and Ben-Zion, 1997; Ben-Zion and Andrews, 1998; Cochard and Rice, 2000; Ben-Zion, 2001; Ben-Zion and Huang, 2002, Shi and Ben-Zion, 2006, Ampuero and Ben-Zion, 2008; Brietzke et al., 2009

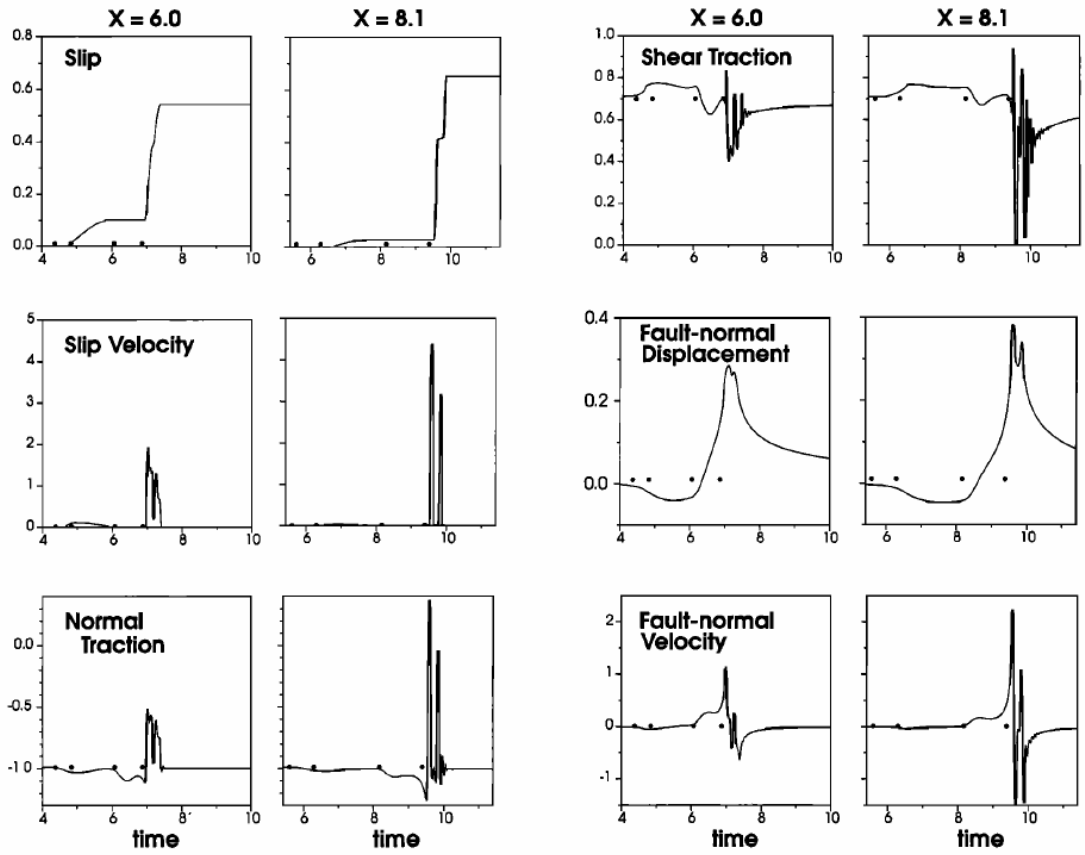

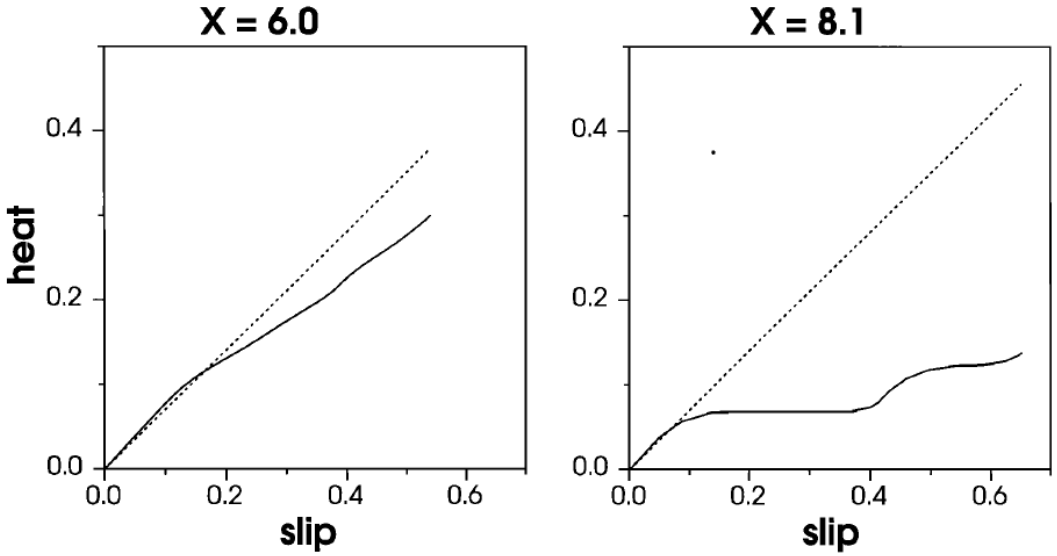

Characteristic features of the wrinkle-like pulse:

1) strong correlation between variations of normal stress and slip

2) strongly asymmetric motion across the fault

3) strongly asymmetric ruptures with a preferred propagation direction

4) self-sharpening with propagation distance

5) evolution to tensional stress (possible fault opening) and little frictional heat

6) evolution to very high slip velocities (e.g.> 10 m/s)

Estimates of slip velocities (Ben-Zion, JMPS 2001)

For a steady-state problem, the frictional criterion $\tau = f\,\sigma$ with Weertman's results for the limiting case $c = c_{GR}$, is

$$\tau^{\infty} = f[\sigma^{\infty} - \mu^*(c_{GR})B] = f[\sigma^{\infty} - \mu^*(c_{GR})v/c_{GR}]$$

The slip velocity inside the pulse adjusts itself to satisfy the above failure criterion and has a value given by

$$v = c_{GR}[\sigma^{\infty} - \tau^{\infty}/f]/\mu^*(c_{GR})$$

For 20% contrast of shear wave velocities, $\sigma^{\infty} \approx$ 150 MPa (1.5 kbar), f = 0.6, and $\tau^{\infty} \approx$ 10-50 MPa (100-500 bar), **get $v \approx$ 15-30 m/s (high but not unrealistic slip velocities!).**

Simulation results with regularized Prakash-Clifton friction (Ben-Zion and Huang, 2002)

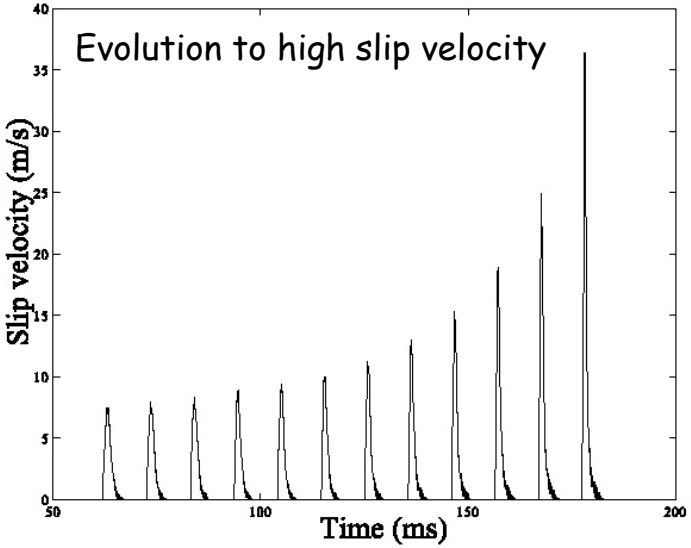

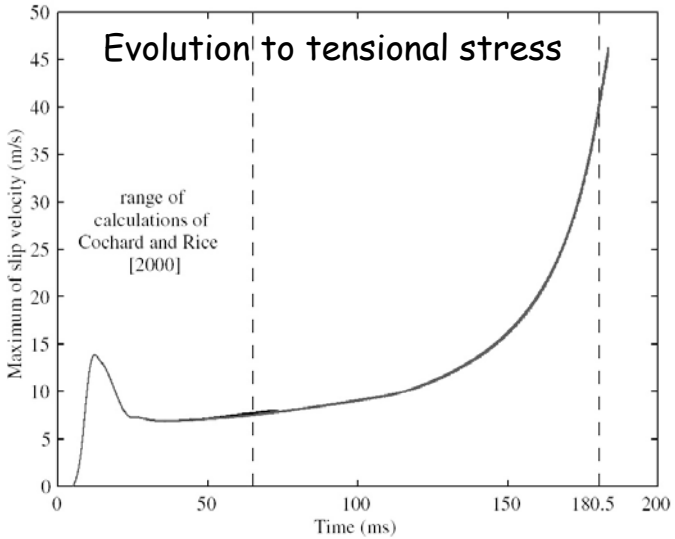

What happens if we add additional ingredients?

- **Stress heterogeneities** (Ben-Zion & Andrews, 1998; Andrews & Harris, 2005)
- **Low-velocity fault zone layer** (Harris & Day, 1997; Ben-Zion & Huang 2002; Brietzke & Ben-Zion, 2006)
- **Viscosity in the bulk** (Harris and Day, 1997; Brietzke and Ben-Zion, 2006)
- **Prakash-Clifton friction** (Cochard & Rice, 2000; Ben-Zion & Huang, 2002)
- **Contrast of permeability structure** (Rudnicki & Rice, 06; Dunham & Rice, 08)
- **Slip-weakening friction** (Harris & Day, 97; Shi & Ben-Zion, 06; Rubin & Ampuero, 2007; Brietzke et al., 2007, 2009)
- **Creation of off-fault damage** (Ben-Zion and Shi, 2005; Duan, 2008)
- **Multiple possible rupture plans** (Brietzke and Ben-Zion, 2006)
- **Velocity-weakening friction** (Ampuero and Ben-Zion, 2008)
- **3D effects** (Brietzke et al., 2007, 2009; Dalguer & Day, 2009)

There is a diversity of phenomena. However, the results show collectively that ruptures evolve for broad ranges of realistic conditions to slip pulses in the preferred direction with the discussed properties.

Slip-weakening friction (Shi and Ben-Zion, 2006)

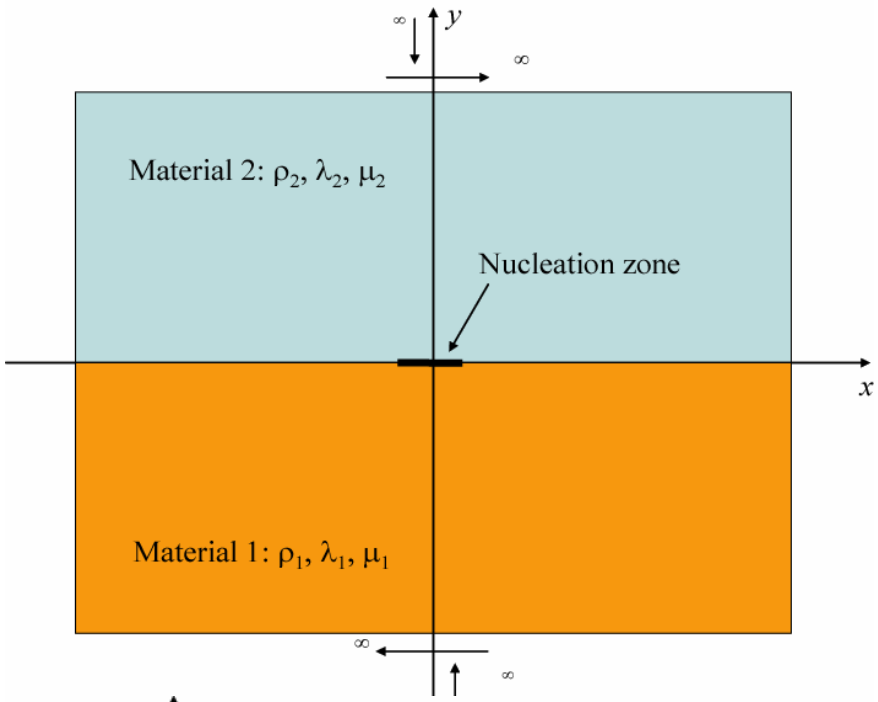

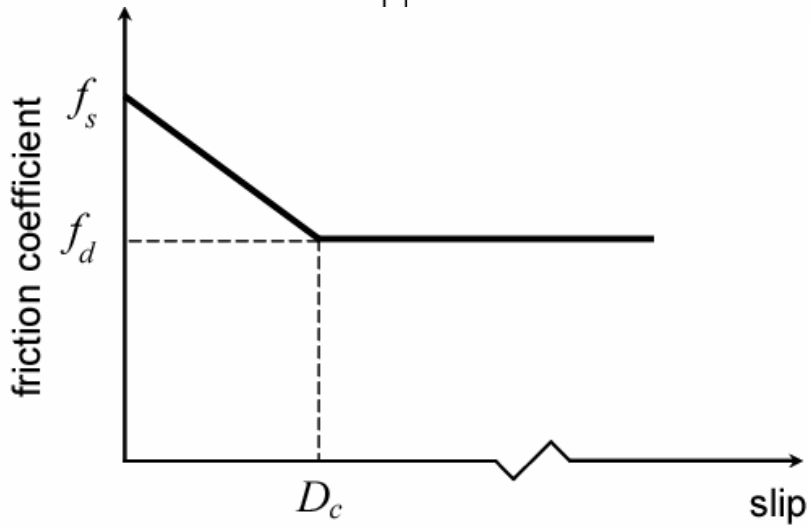

Strong small nucleation phase corresponding to failure of a strong asperity

Parameter space study for different values of

- $f_s - f_d$
- $f_s\sigma - \tau_0$
- velocity contrast

$f_s - f_d = 0.1$; $f_s\sigma - \tau_0 = 9$ MPa

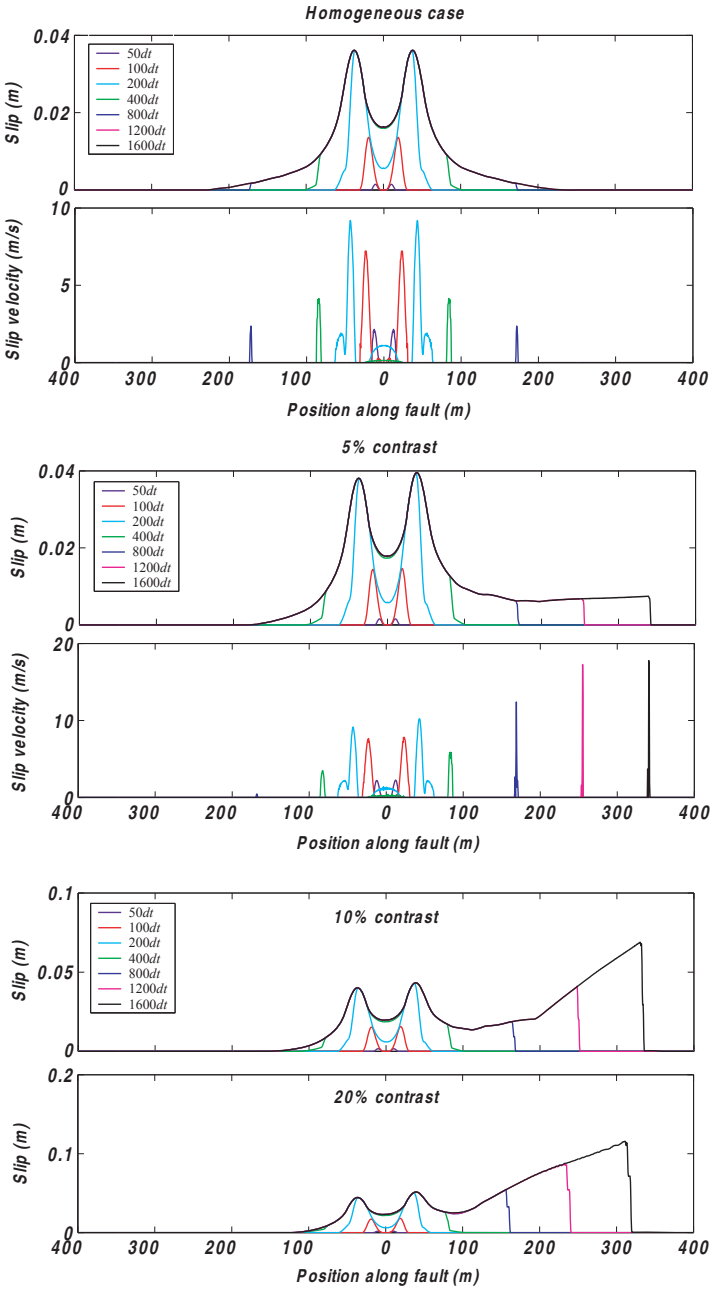

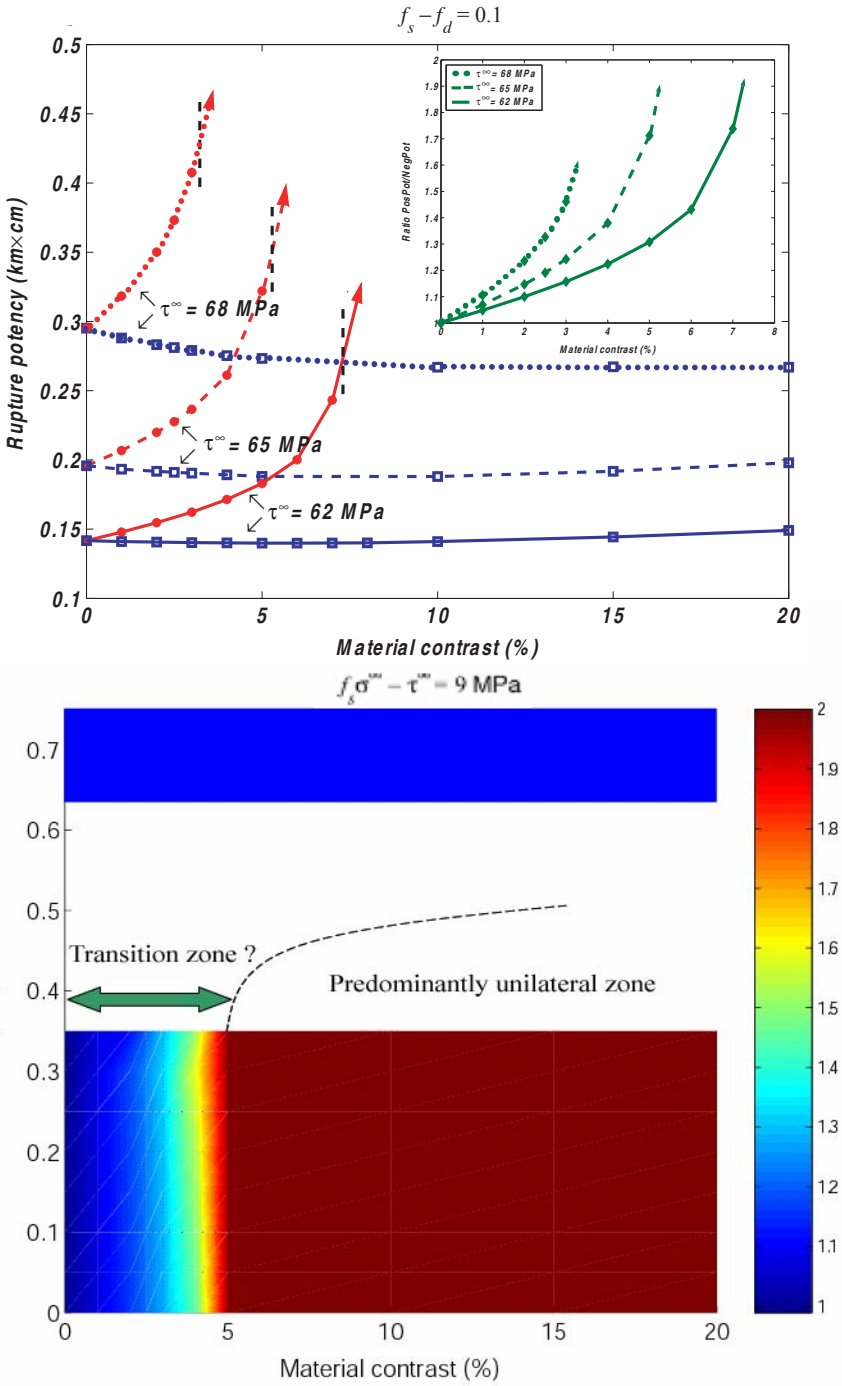

Simulations with imposed super-shear rupture in the nucleation zone can excite also a weak super-shear pulse in the opposite direction

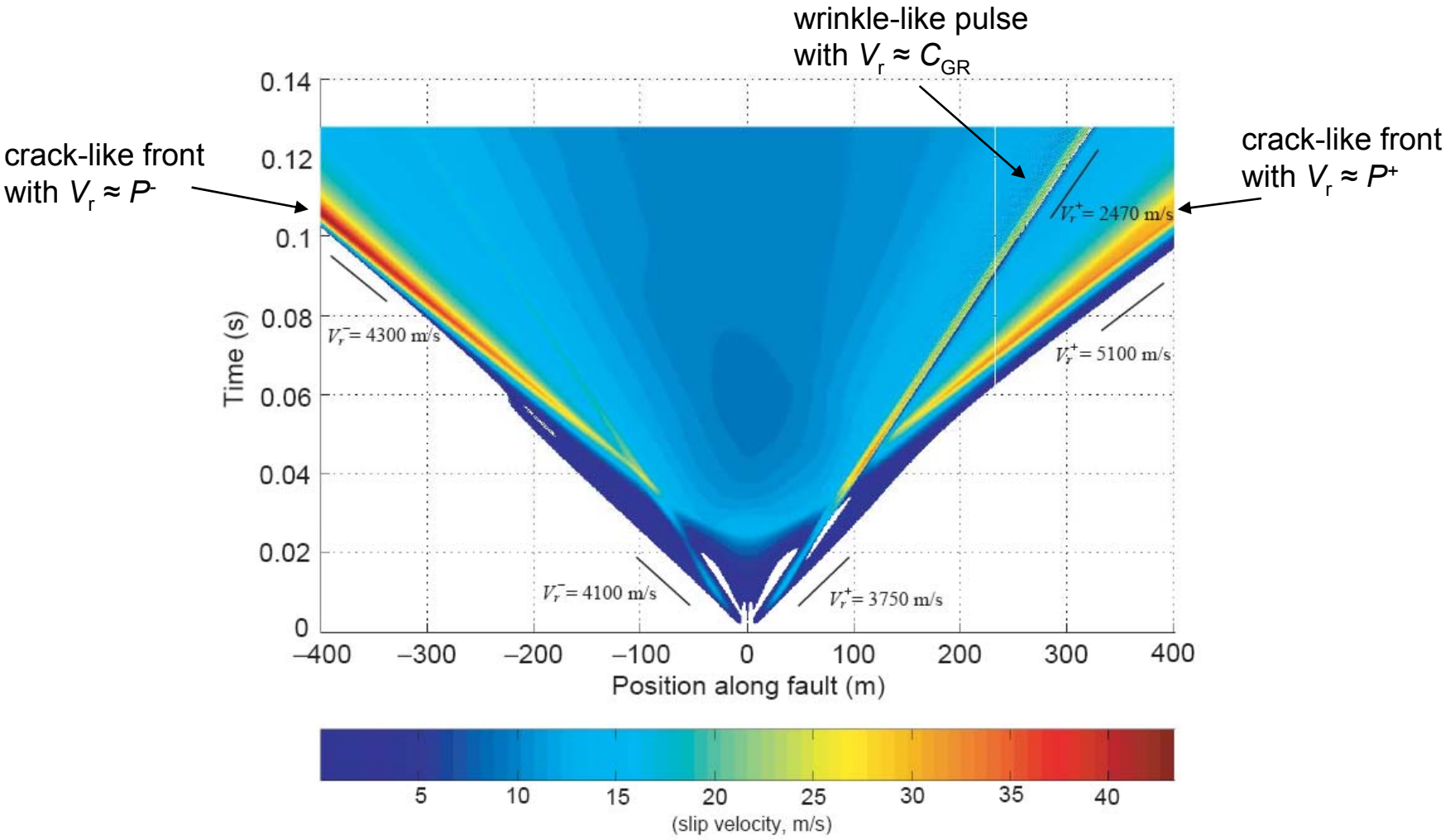

Bimaterial ruptures with slip- and velocity-dependent friction and stress heterogeneities (Ampuero and Ben-Zion, GJI 2008)

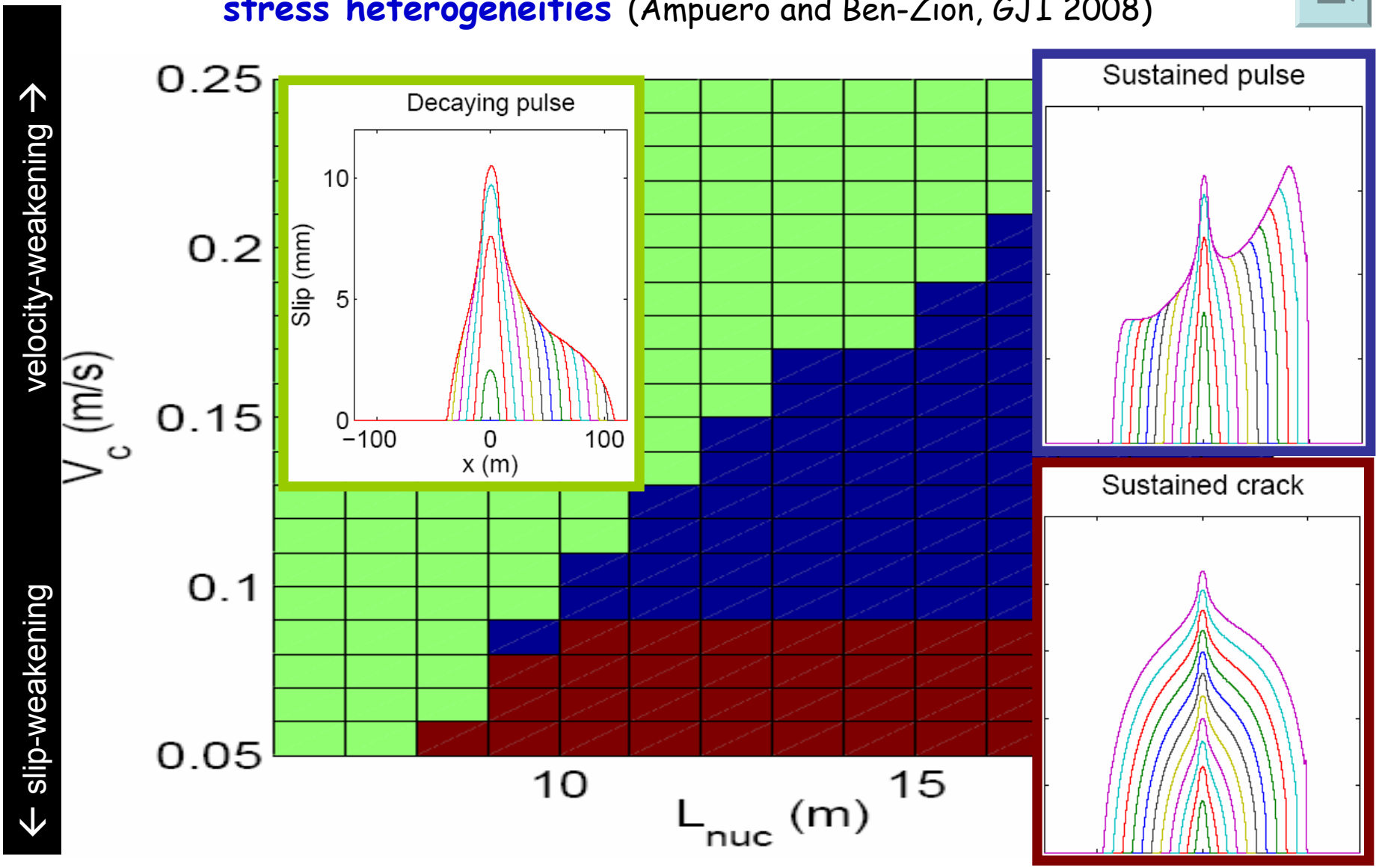

The dynamic changes of σ produce asymmetric crack-tip fields
Cases leading to pulses have pronounced macroscopic asymmetry

The results are robust with respect to stress heterogeneities
(and also proxy for off-fault yielding)

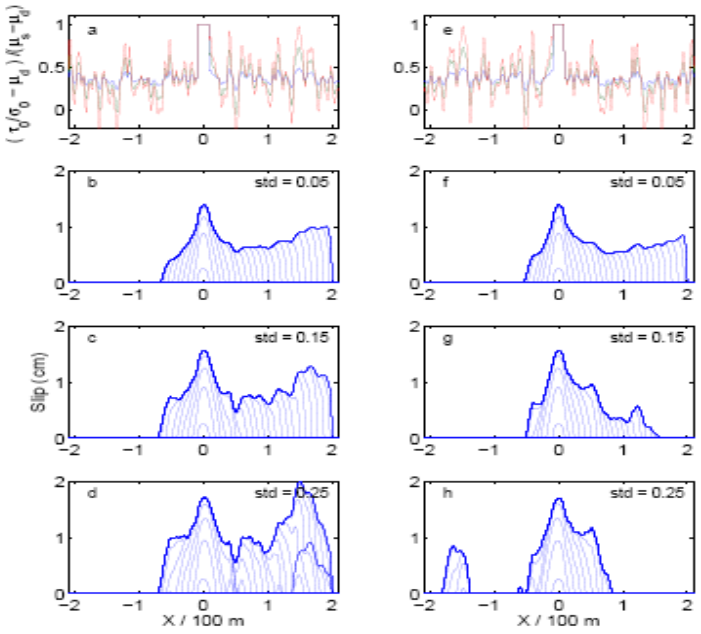

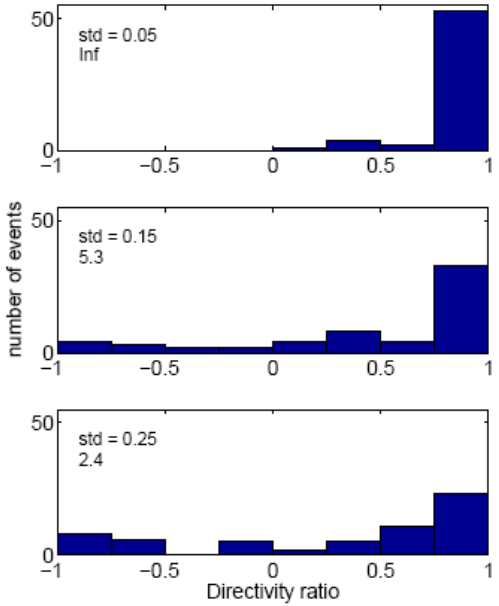

Figure 16. Histograms of the directivity ratio ($DR = \pm 1$ indicates strong asymmetry in the "preferred" and opposite rupture direction, respectively) in bimaterial ruptures with heterogeneous initial stress, for three values of std (indicated in each plot, normalized by the nominal strength drop $\sigma_0(\mu_s - \mu_d)$). The ratio of the number of events with $DR > 0.5$ to the number of events with $DR < -0.5$ is also indicated below std.

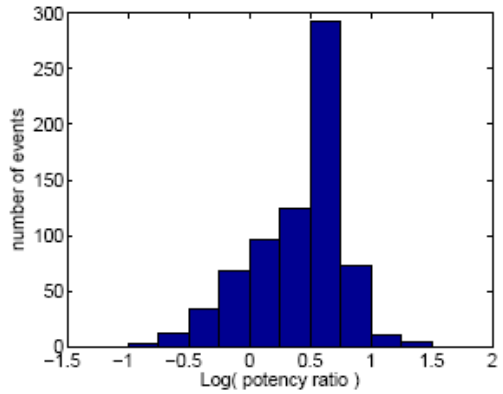

Bimaterial ruptures are likely to have

- **Strong directivity**
- **Strong reduction of σ at crack tip (and hence large amount of high frequency radiation)**

Bimaterial ruptures with slip-weakening and stress heterogeneities in 3D

(Brietzke, Cochard and Igel, GJI 2009)

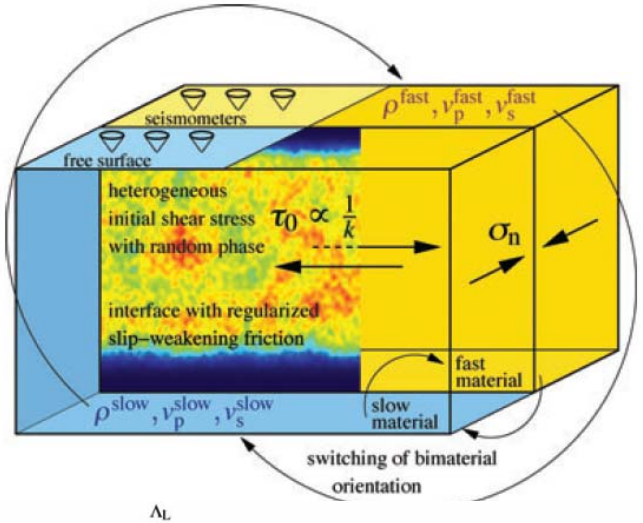

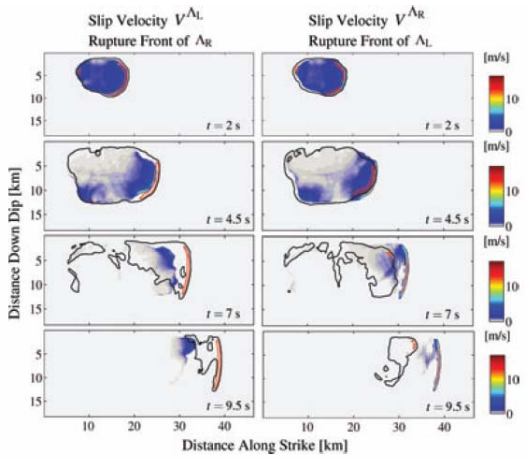

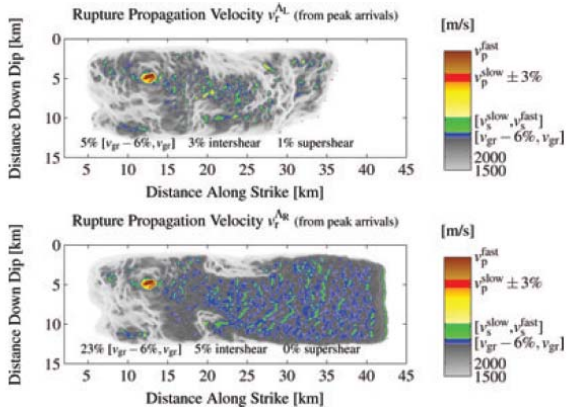

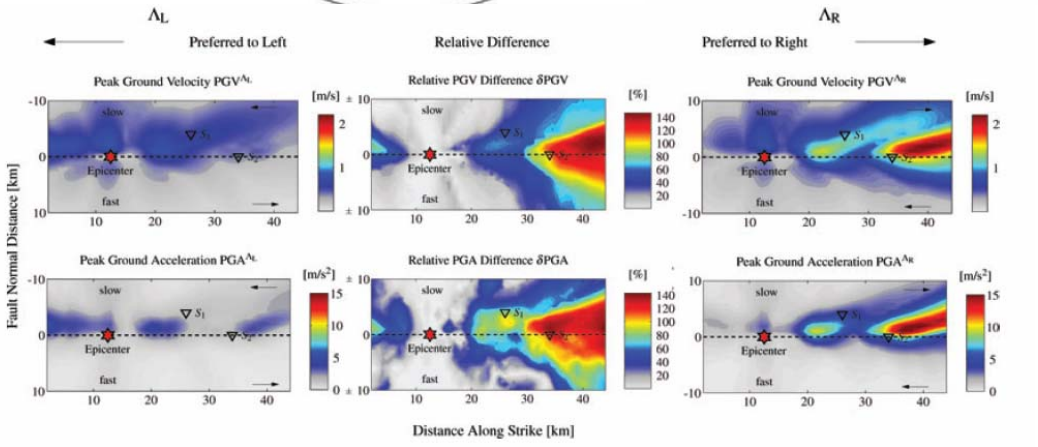

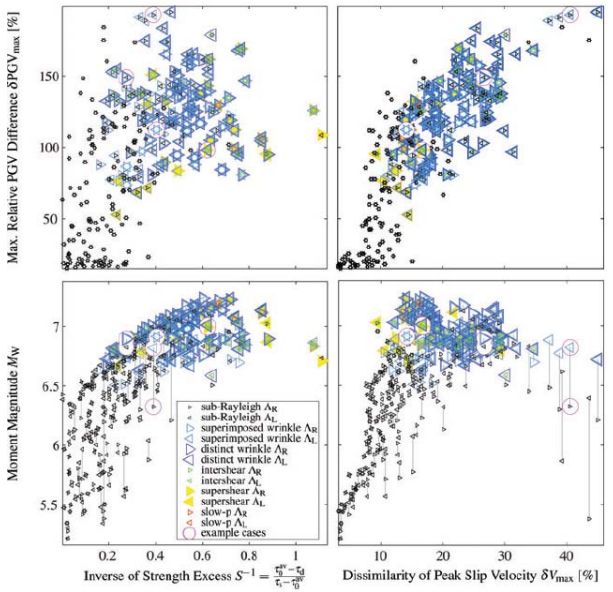

Figure 18. Summary showing the occurrence of the six possible propagation modes, as a function of inverse of strength excess, dissimilarity of peak slip velocity, moment magnitude, and maximum relative PGV difference for 266 simulation pairs.

- The rupture propagation and radiations are significantly influenced by the material contrast.

- Many cases produce strongly asymmetric ruptures with narrow wrinkle-like pulses and enhanced high frequency radiation.

Relations to field observations?

Need data associated with many earthquakes

Henry and Das (2001), McGuire et al. (2002): analysis of >100 large earthquakes shows that most are predominantly unilateral.

These earthquakes propagate on large but different fault zones!

Large data sets associated with single fault zones:

Dor et al. (2006a,b, 2008), Lewis et al. (2005, 2007), Wechsler et al. (2009): strong asymmetry of rock damage in the structures of the SAF, SJF and NAF. Clear but indirect evidence.

Rubin and Gillard (2000), Zaliapin and Ben-Zion (2009): strong asymmetry of dynamic triggering (early aftershocks) on the SAF and other large faults. Clear but still indirect signal.

Direct evidence requires high-resolution high-frequency seismology!

Expected damage patterns generated by many earthquakes

Dynamic rupture with generation of damage in the bulk

Homogenous solid

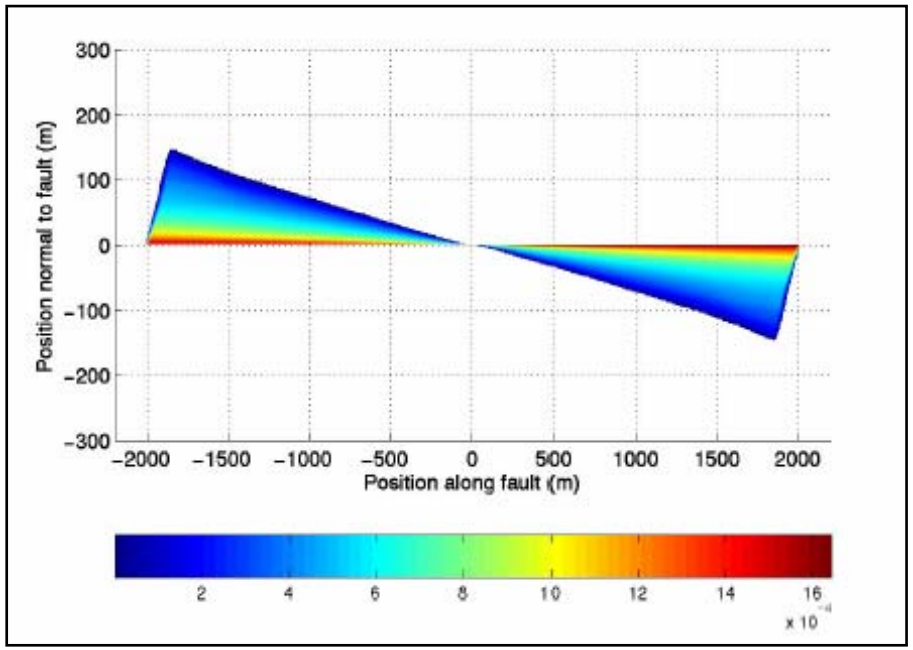

Andrews, 2005

Bimaterial

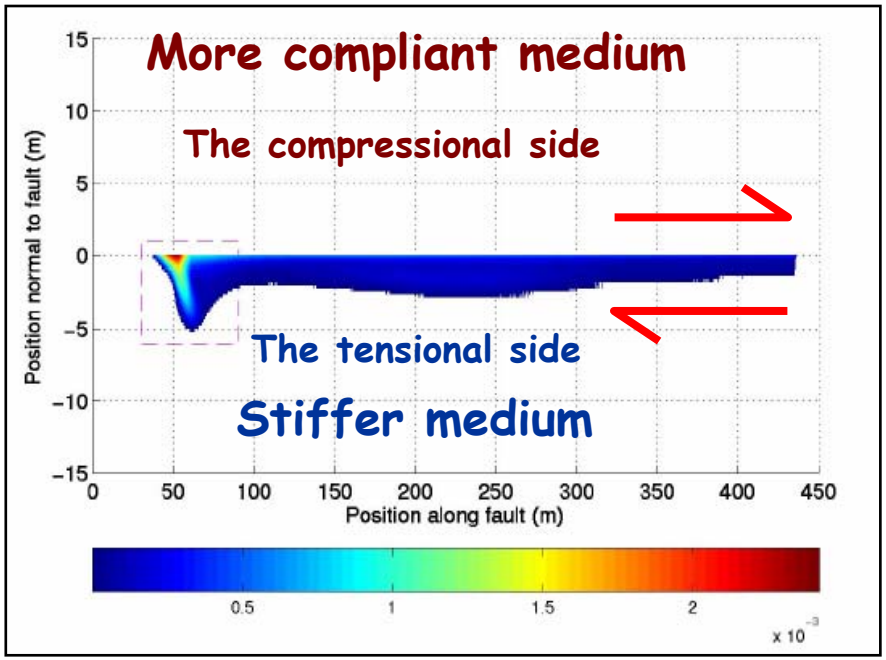

Ben-Zion and Shi, 2005

Damage generation for different depth conditions

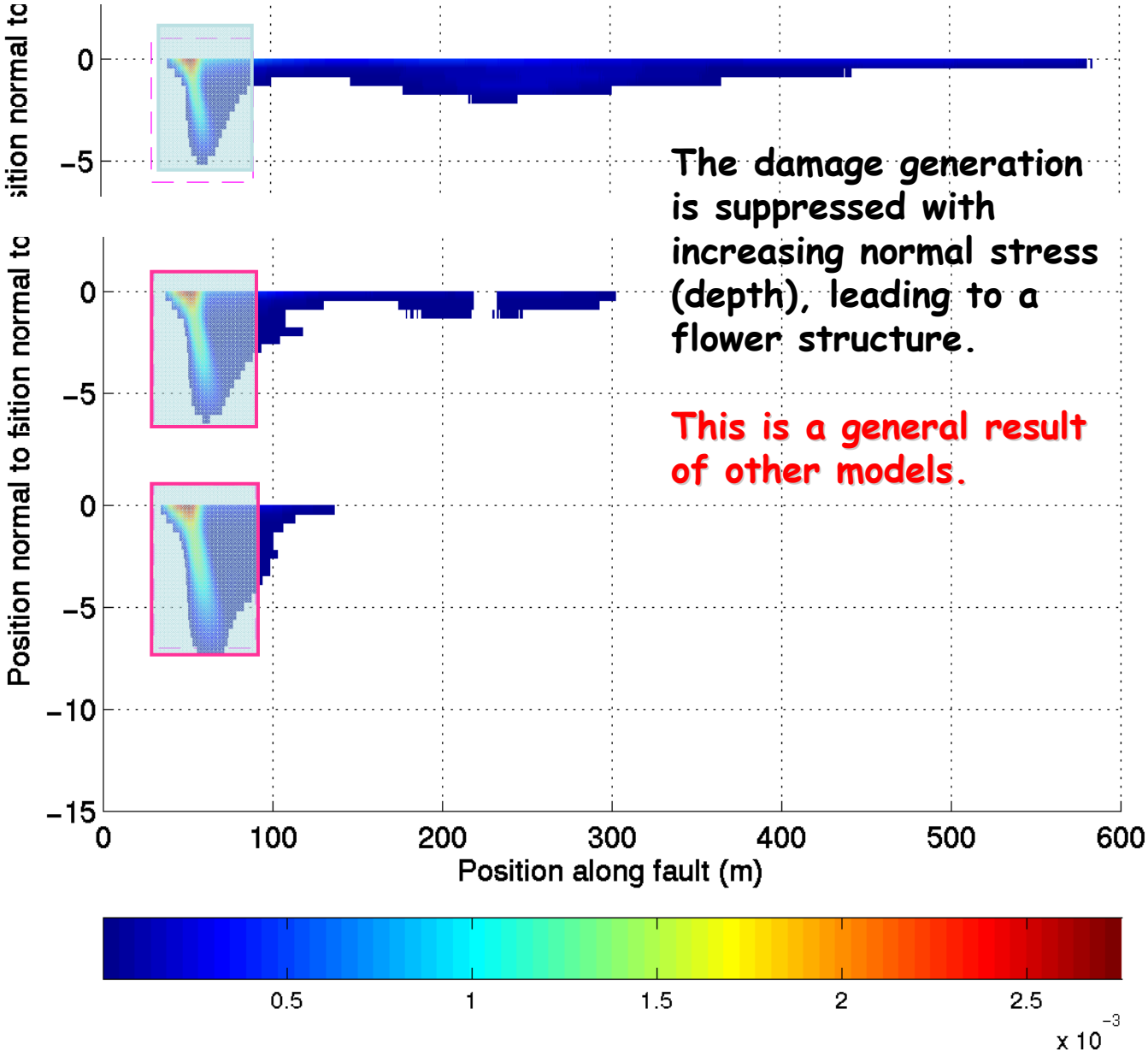

The damage generation is suppressed with increasing normal stress (depth), leading to a flower structure.

This is a general result of other models.

3 km

5 km

7 km

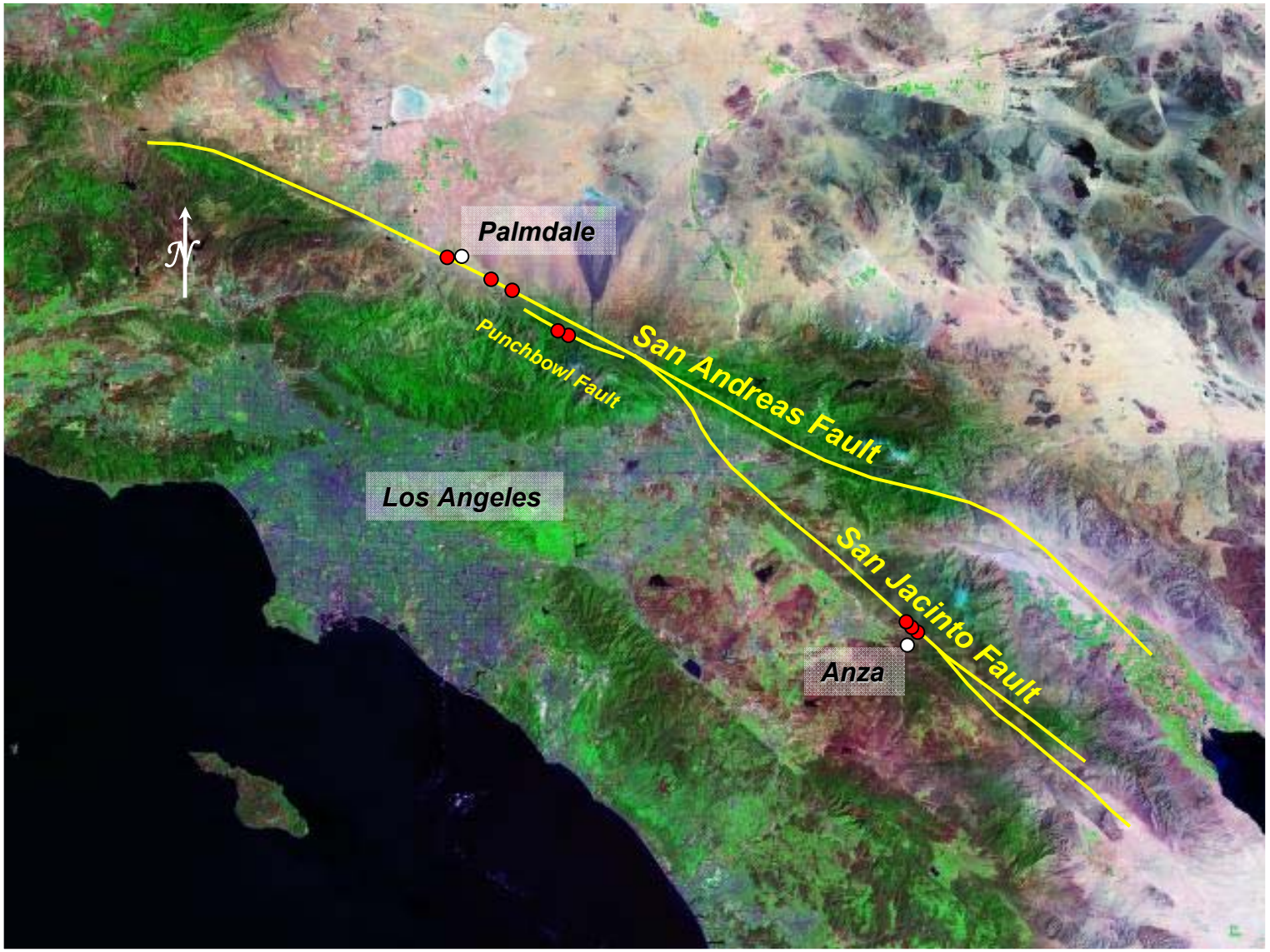

Dor, Ben-Zion, Rockwell, Brune (PAGEOPH, 2006, EPSL, 2006)

SJF near Anza

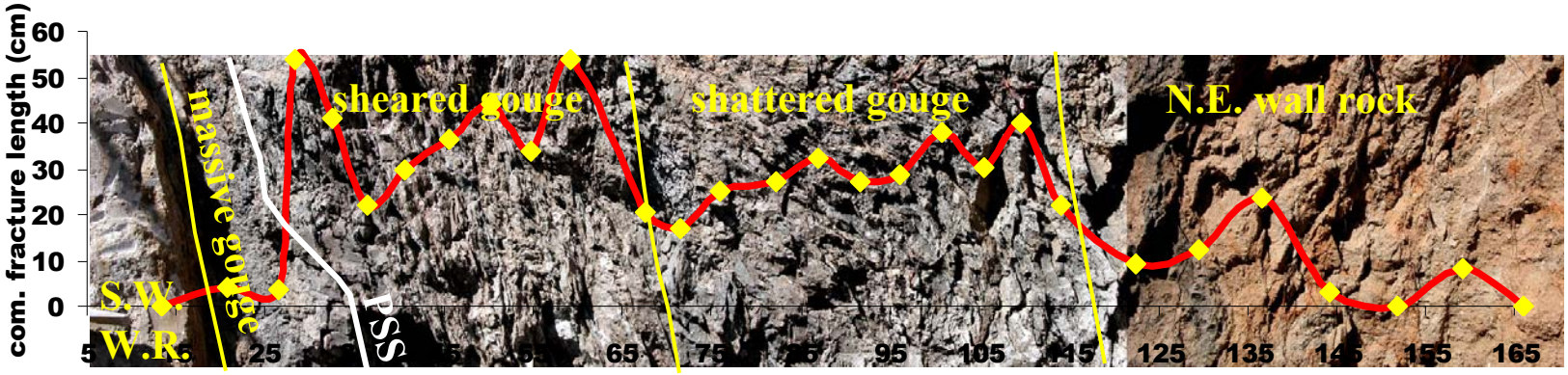

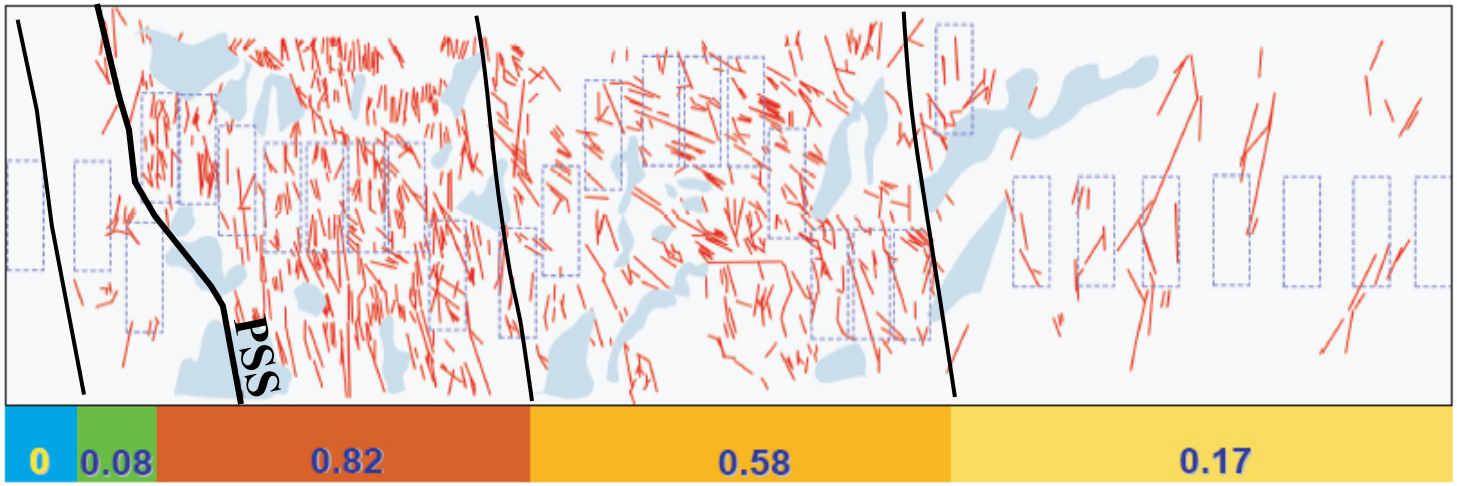

Gouge scale ~1m

Dor et al. (PAGEOPH, 2006)

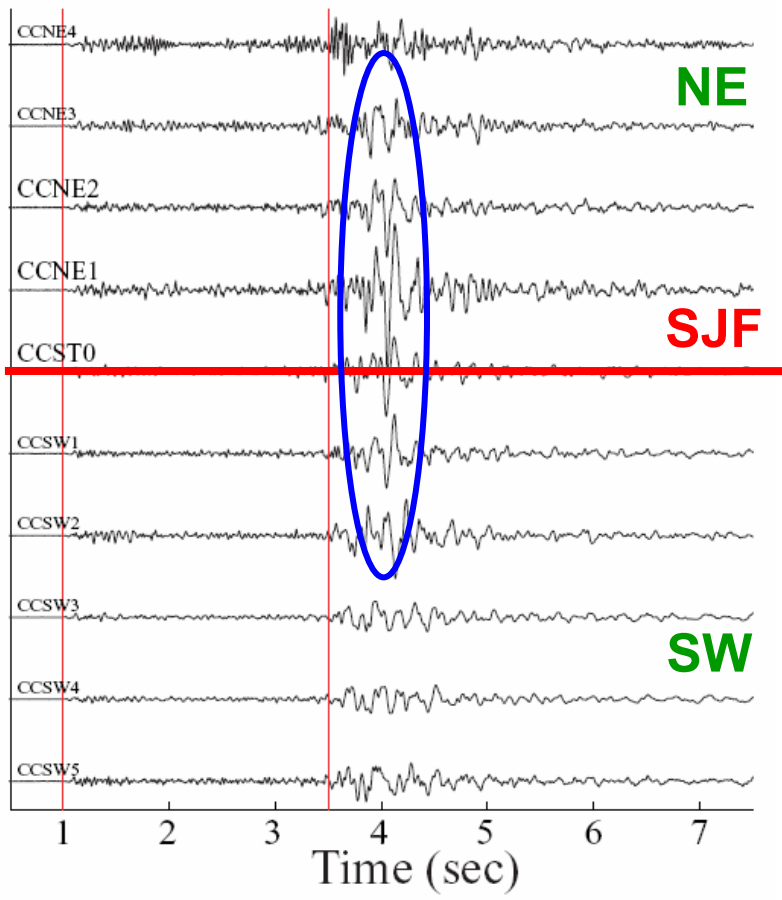

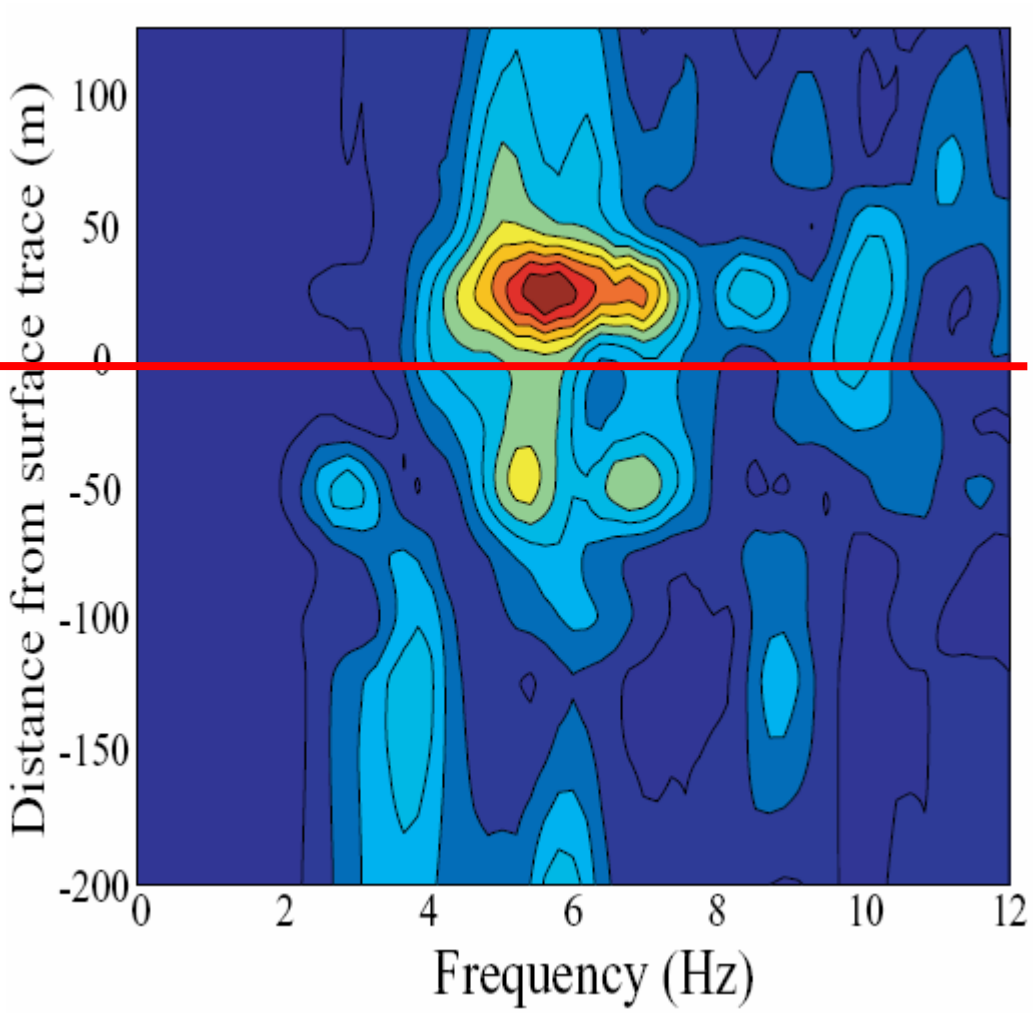

Damage zone scale

Lewis et al. (GJI 2005)

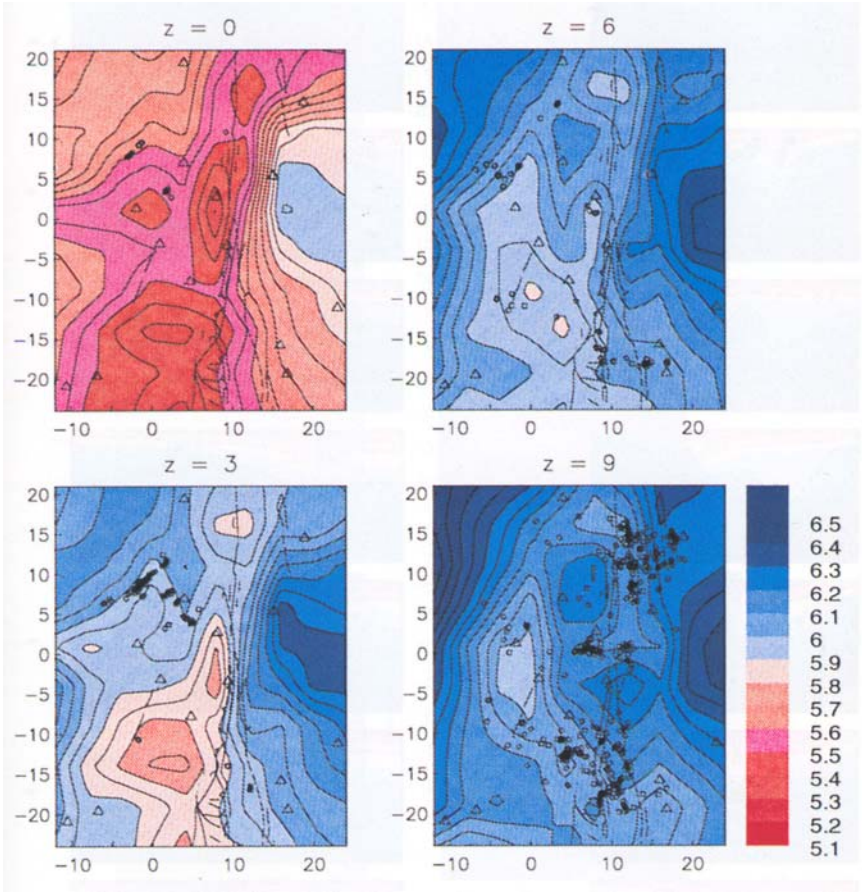

Scott et al. (1994)

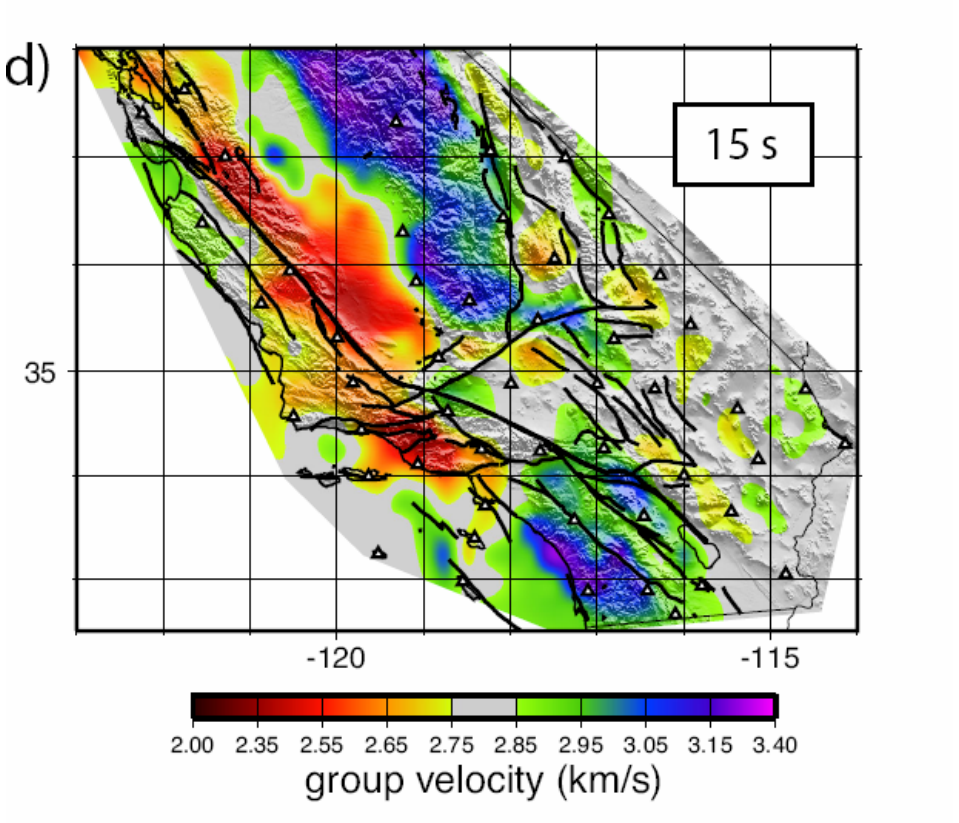

Shapiro et al. (2005)

SAF near Palmdale

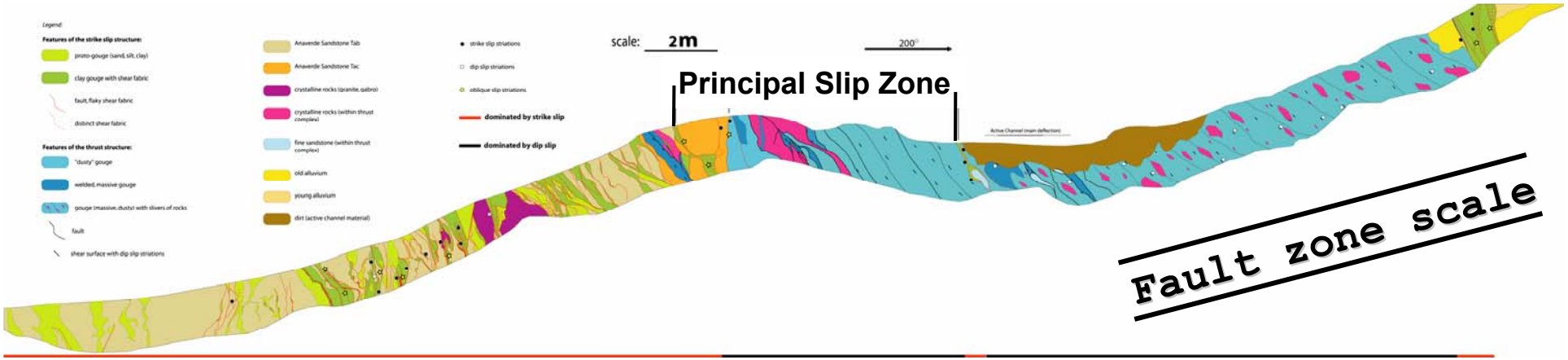

Dor et al., PAGEOPH, 2006

Pulverized rocks in the Mojave section of the SAF

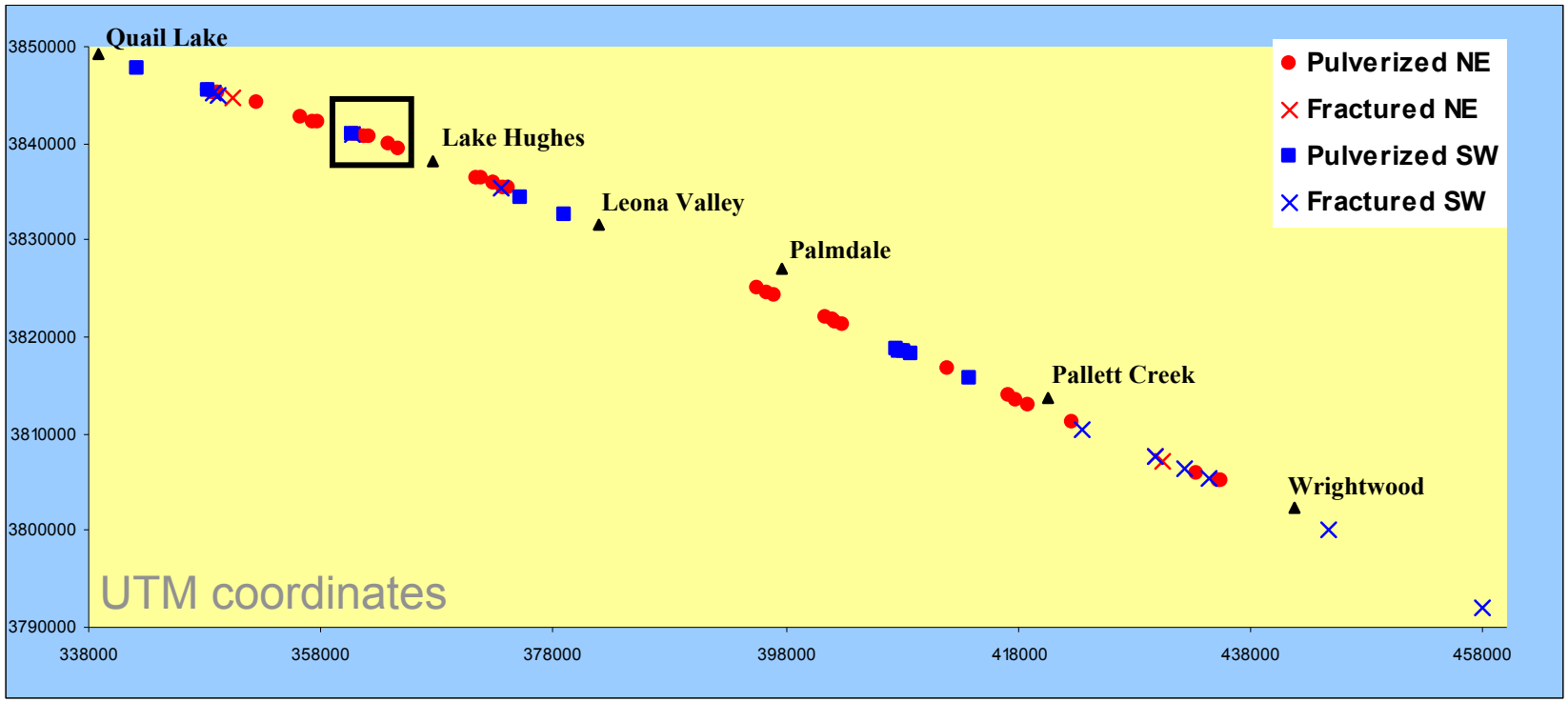

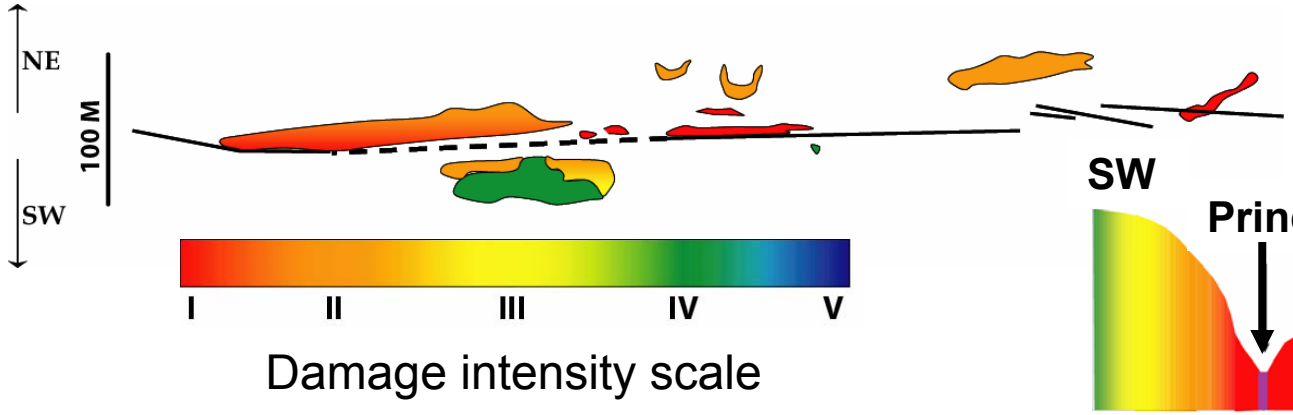

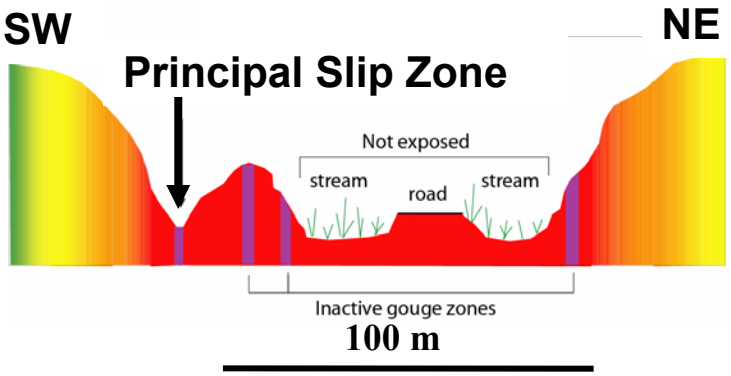

Dor et al., EPSL, 2006

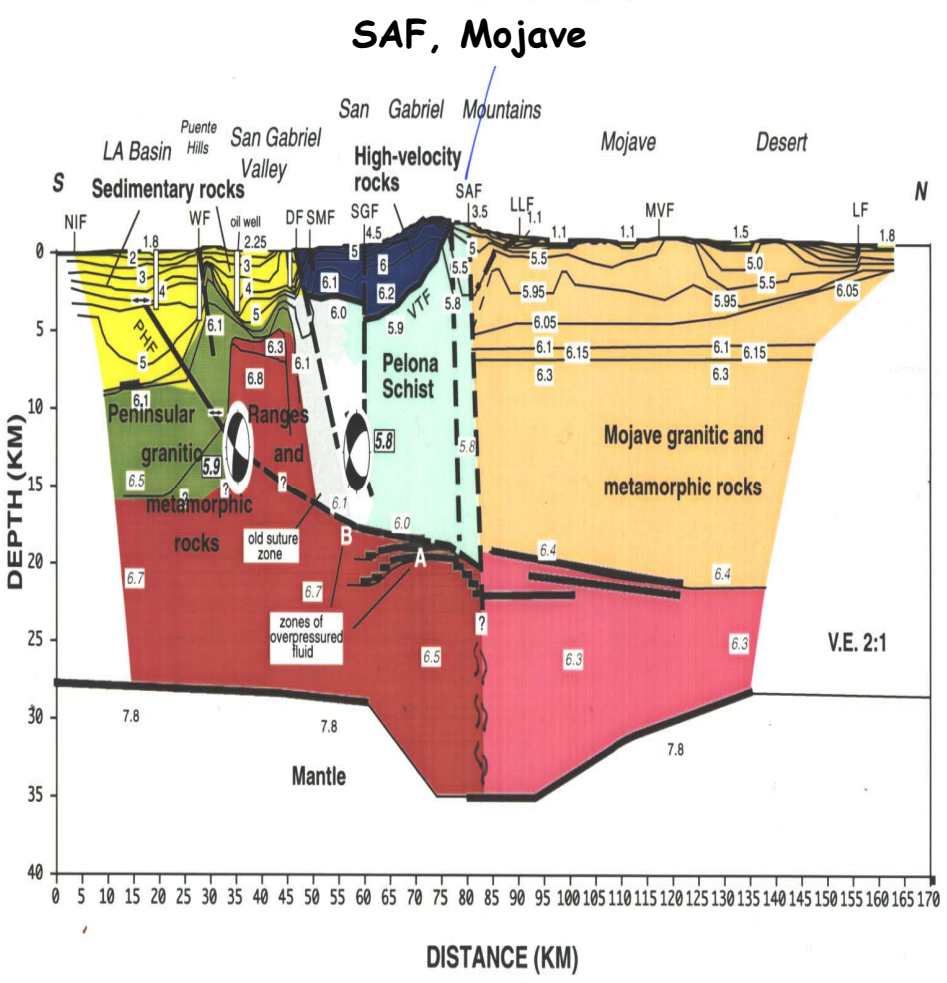

Fuis et al. (2003)

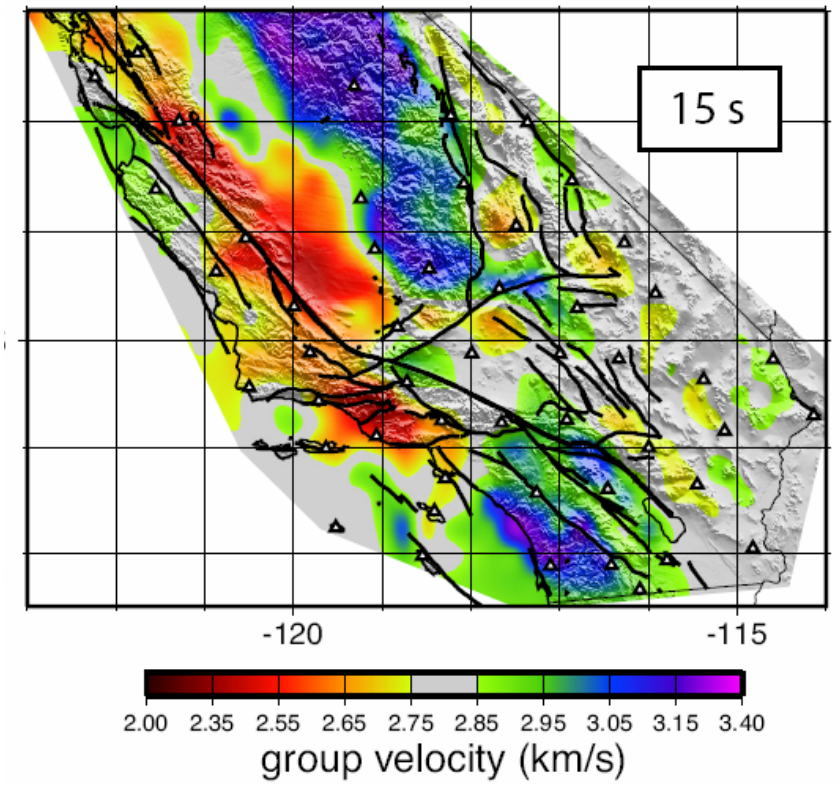

Shapiro et al. (2005)

Asymmetric dynamic earthquake triggering along strike

(Rubin and Gillard, 2000; Rubin, 2002)

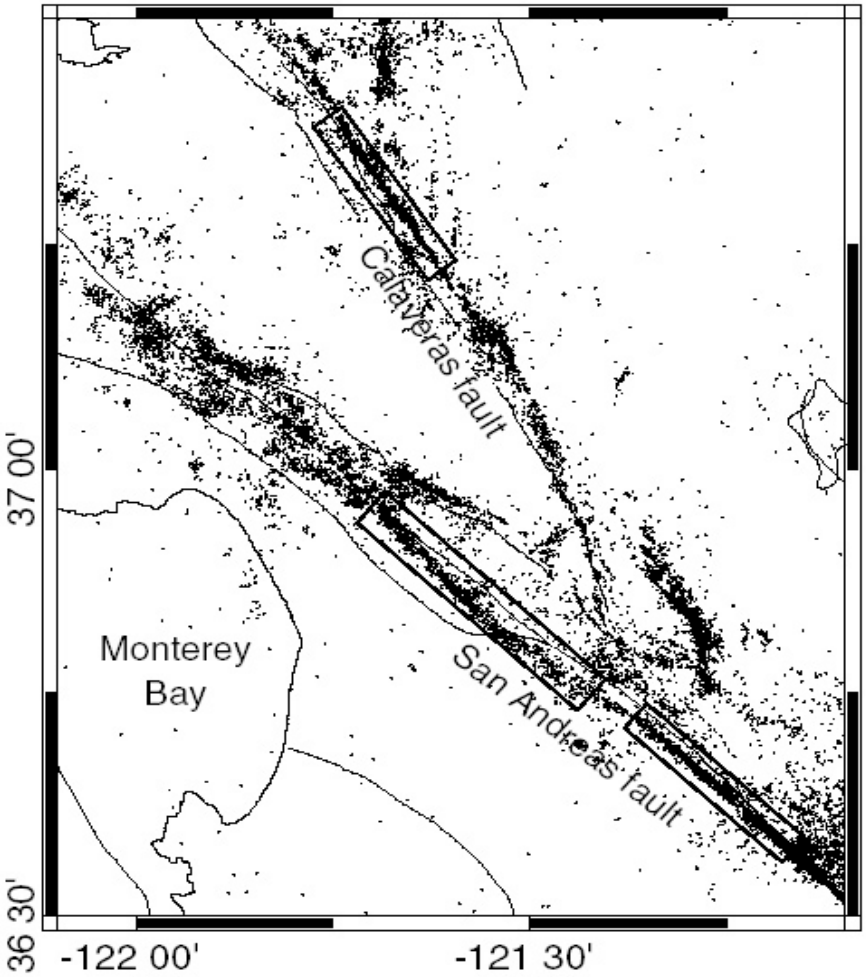

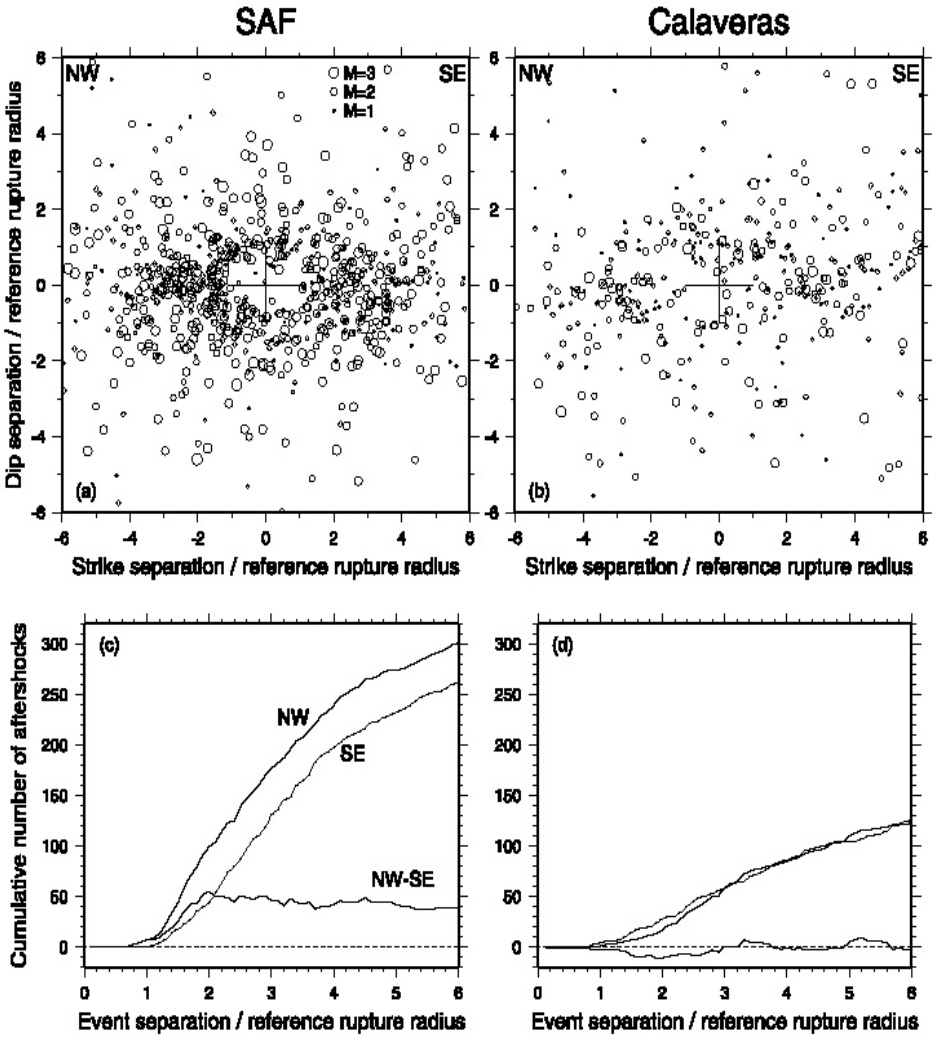

Zaliapin and Ben-Zion (2009)

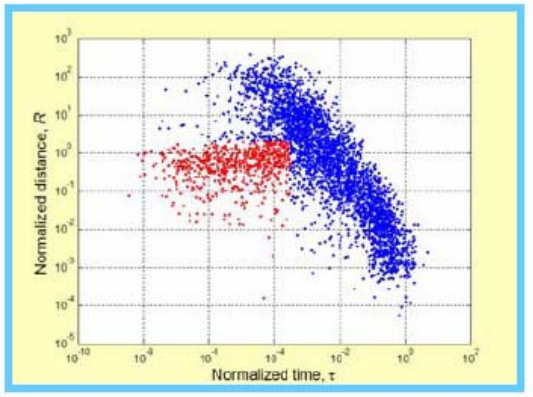

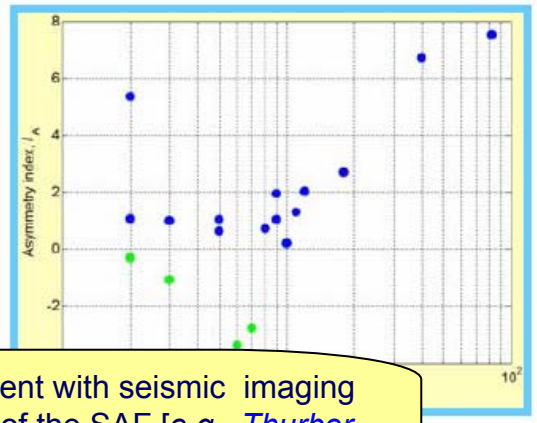

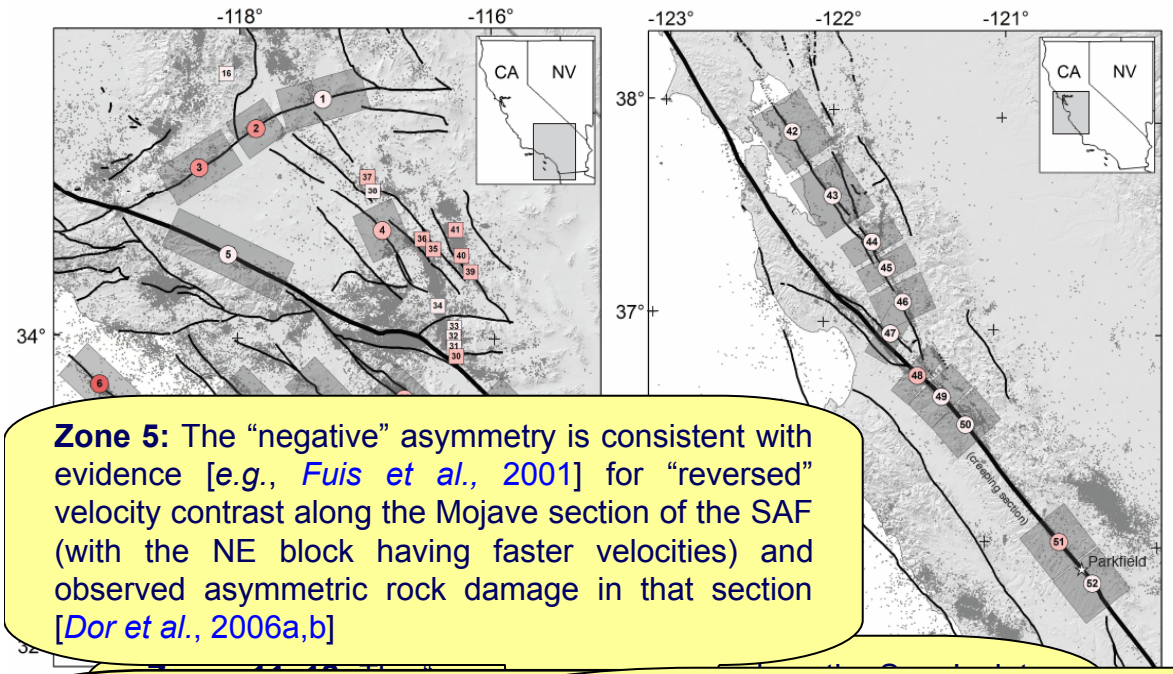

Zone 5: The "negative" asymmetry is consistent with evidence [*e.g.*, *Fuis et al.*, 2001] for "reversed" velocity contrast along the Mojave section of the SAF (with the NE block having faster velocities) and observed asymmetric rock damage in that section [*Dor et al.*, 2006a,b]

Zone 1: The lack of significa
consistent with the lack of pro
contrast across the eastern

Zones 48, 51: The "positive" asymmetry is consistent with seismic imaging of the velocity contrast along the Parkfield section of the SAF [*e.g.*, *Thurber et al.*, 2006; *Ben-Zion et al.*, 1992]. The results in zone 48 to the left are consistent with similar findings of *Rubin and Gillard* [2000].

or zone 51

netry is seen e Ellsinore fault (zone 12)

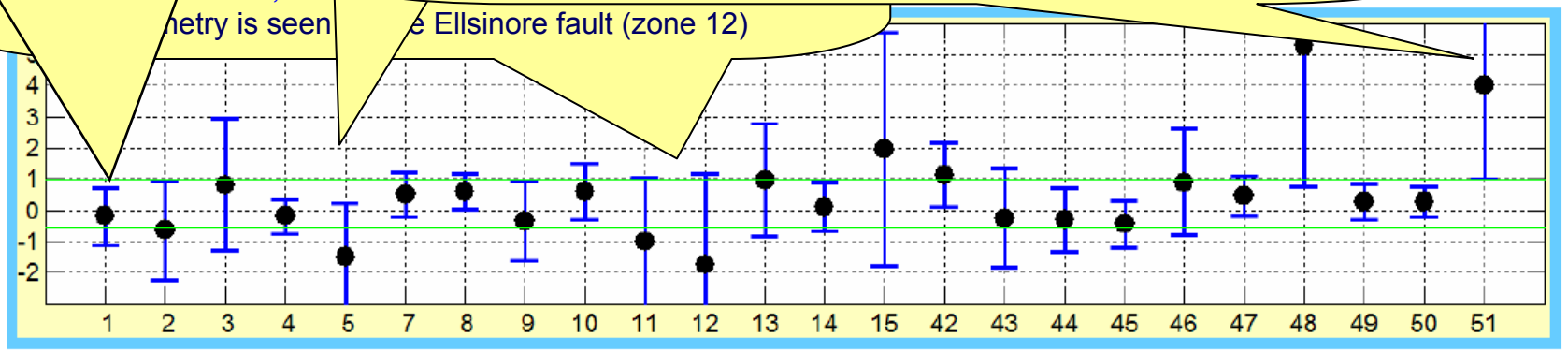

Asymmetry results for different fault zones

Conclusions II

- Ruptures along a bimaterial interface evolve for ranges of realistic conditions to narrow pulses with preferred propagation direction, high slip velocity, and possible transient fault opening near the rupture tip.

- Such properties can have fundamental implications to many basic (earthquake physics) and practical (shaking hazard estimates) aspects of earthquake seismology.

- The cumulative effect of such ruptures is expected to produce asymmetric damage pattern across the fault in the top few km.

- Multi-scale multi-signal geological mapping show strongly asymmetric damage in the structures of the San Jacinto, Punchbowl, San Andreas and North Anatolian faults, which correlate with available information on the velocity structures at depth as predicted for ruptures on a bimaterial interface.

- Analyses of trapped waves in the San Jacinto fault near Anza and head waves in the San Andreas fault near Hollister show asymmetric damage zone in the ~3.5 km, with more damage on the predicted sides of the faults.

- Analyses of dynamic triggering patterns along several sections of the SAF and SJF indicate clear asymmetries, compatible with statistically-preferred propagation directions as predicted by for the local velocity models.

- More direct tests requires high-resolution high-frequency seismology!!!